Earthquakes and Structures, *Vol. 11, No. 5 (2016) 741-777*
DOI: http://dx.doi.org/10.12989/eas.2016.11.5.741

Simplified elastic design checks for torsionally balanced and unbalanced low-medium rise buildings in lower seismicity regions

Nelson T.K. Lam*[1,3], John L. Wilson[2,3a] and Elisa Lumantarna[1,3b]

[1]*Department of Infrastructure Engineering, The University of Melbourne, Parkville, Victoria, Australia*
[2]*Faculty of Science, Engineering and Technology, Swinburne University of Technology, Melbourne, Victoria, Australia*
[3]*Bushfire and Natural Hazards Cooperative Research Centre, Melbourne Australia*

(Received February 8, 2016, Revised October 7, 2016, Accepted October 11, 2016)

Abstract. A simplified approach of assessing torsionally balanced (TB) and torsionally unbalanced (TU) low-medium rise buildings of up to 30 m in height is presented in this paper for regions of low-to-moderate seismicity. The *Generalised Force Method of Analysis* for TB buildings which is illustrated in the early part of the paper involves calculation of the deflection profile of the building in a 2D analysis in order that a capacity diagram can be constructed to intercept with the acceleration-displacement response spectrum diagram representing seismic actions. This approach of calculation on the planar model of a building which involves applying lateral forces to the building (waiving away the need of a dynamic analysis and yet obtaining similar results) has been adapted for determining the deflection behaviour of a TU building in the later part of the paper. Another key original contribution to knowledge is taking into account the strong dependence of the torsional response behaviour of the building on the periodic properties of the applied excitations in relation to the natural periods of vibration of the building. Many of the trends presented are not reflected in provisions of major codes of practices for the seismic design of buildings. The deflection behaviour of the building in response to displacement controlled (DC) excitations is in stark contrast to behaviour in acceleration controlled (AC), or velocity controlled (VC), conditions, and is much easier to generalise. Although DC conditions are rare with buildings not exceeding 30 m in height displacement estimates based on such conditions can be taken as upper bound estimates in order that a conservative prediction of the displacement profile at the edge of a TU building can be obtained conveniently by the use of a constant amplification factor to scale results from planar analysis.

Keywords: torsion; torsionally unbalanced; asymmetric building; low-medium rise building; low seismicity

1. Introduction

*Corresponding author, Associate Professor, E-mail: ntkl@unimelb.edu.au
[a]Professor, E-mail: jwilson@swin.edu.au
[b]Lecturer, E-mail: elu@unimelb.edu.au

http://www.techno-press.com/journals/eas&subpage=7 ISSN: 2092-7614 (Print), 2092-7622 (Online)

Contemporary seismic codes of practice including Eurocode 8 (EN 1998-1 2004) considers dynamic analysis to be the (default) reference method of assessment of structural response behaviour given that most commercial structural analyses packages which are widely available worldwide have a structural dynamics analysis capability. The number of structural engineers who are involved in designing structures for earthquakes is increasing as more countries are becoming urbanised and are introducing seismic design codes of practice to manage the risk. However, many engineers are not knowledgeable with the fundamentals of structural dynamics and do not possess adequate analytical skills to perform such dynamic analyses.

A traditional method of analysis namely the lateral force method (terminology used by Eurocode 8 (EN 1998-1 2004)) was originally developed to offer designers an option to simplify the analysis of the building by the use of prescribed equivalent static forces to emulate seismic actions. Building structures that may be analysed by such a prescriptive procedure would need to fulfil very stringent requirements on vertical and horizontal regularity. Consequently, this lateral force method as stipulated by codes of practices cannot be applied to the great majority of building structures in practice.

Alternative viable simple techniques of assessment in support of numerically intensive computations are in demand given that a simplified behavioural model is able to: (i) provide independent, and reliable, predictions and (ii) foster a better understanding of the fundamentals and portray behavioural trends to guide preliminary design.

In regions of low-to-moderate seismicity the design and analysis of building structures within the framework of the current codes of practices are typically based on linear elastic behaviour when the behaviour factor, or structural modification factor, is used to take into account the capacity reserve in the structure when excited beyond the yield limit. The simplified methods of analysis to be introduced in this paper are aimed at approximating results from analyses as required by the code assuming elastic response behaviour of both torsionally balanced (TB) and torsionally unbalanced (TU) building structures.

The simplified methods to be introduced herein involves representing earthquake ground motions in the acceleration, velocity and displacement formats, and the acceleration-displacement response spectrum (ADRS) diagram (Section 2). The code lateral force method has been extended to incorporate the use of the ADRS diagram to achieve improved accuracies of the estimated seismic actions on a TB building structure. The introduced method of analysis is given the name: *Generalised Force Method* of analysis. A nine-storey building supported by a frame-wall system is used as an example for illustration (Section 3). This planar analysis approach has been adapted for determining the deflection behaviour of a TU building at the critical edge (Section 4) and finally, the introduced analysis method is verified by the use of a worked example (Section 5).

2. Response spectrum presented in different formats

Response spectrum models which are usually presented by codes of practices for the structural design of buildings are normally presented in the acceleration format which shows the correlation of the response spectral acceleration demand (of single-degree-of-freedom systems possessing 5% critical damping) with their natural period of vibration. The commonly adopted response spectrum format of the flat-hyperbolic form has since been further developed by many major codes of practices (AS1170.4 2007, NZS1170.5 2004, EN 1998-1 2004) into three zones as presented schematically in Fig. 1(a). This three zone response spectrum model can be parameterised in terms

of the maxima of the response spectral acceleration (RSA_{max}), response spectral velocity (RSV_{max}) and response spectral displacement (RSD_{max}) as shown schematically in Fig. 1(b). Values of these parameters can be obtained from several well publicised attenuation models for shallow earthquakes that have been developed for worldwide applications (Abrahamson *et al.* 2014, Boore and Atkinson 2014, Campbell and Bozorgnia 2014, Chiou and Youngs 2014, PEER 2015). The transformation of the response spectrum between the acceleration, velocity and displacement formats are summarised in Fig. 2 whilst the construction of the acceleration-displacement response spectrum format (which is also known as the ADRS diagram) is illustrated Fig. 3 (refer Wilson and Lam (2006) and Lam and Wilson (2004) for more detailed descriptions). The ADRS diagram is employed in the modified lateral force method for obtaining an improved estimate of the acceleration and displacement demand on the structure in the following section.

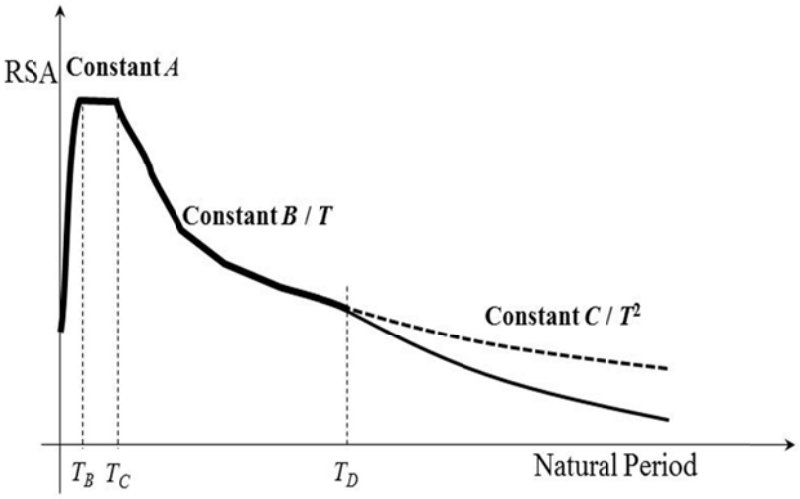

(a) Typical code format

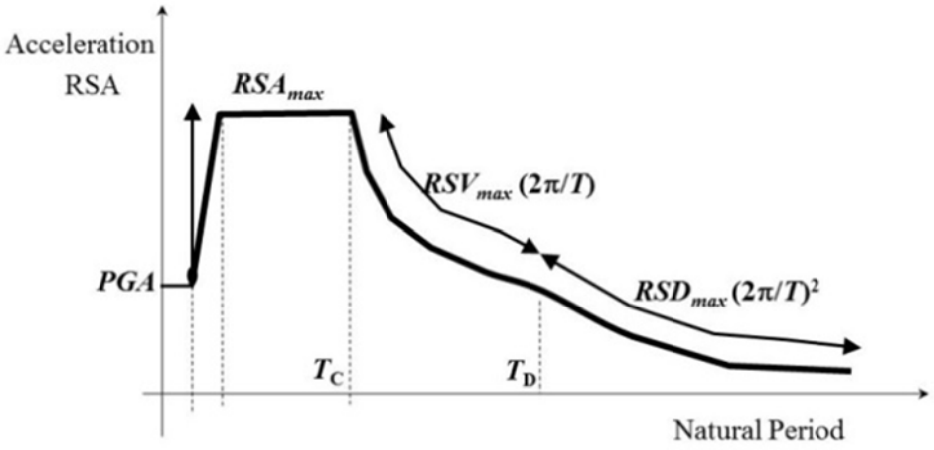

(b) Response spectral maxima parameterisation

Fig. 1 The three zones of a design response spectrum

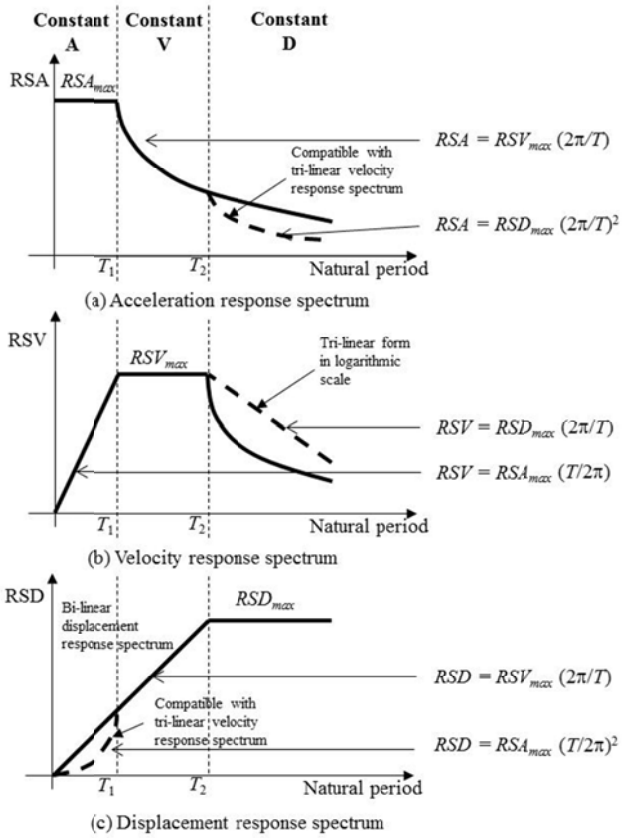

Fig. 2 Response spectrum in acceleration, velocity and displacement formats

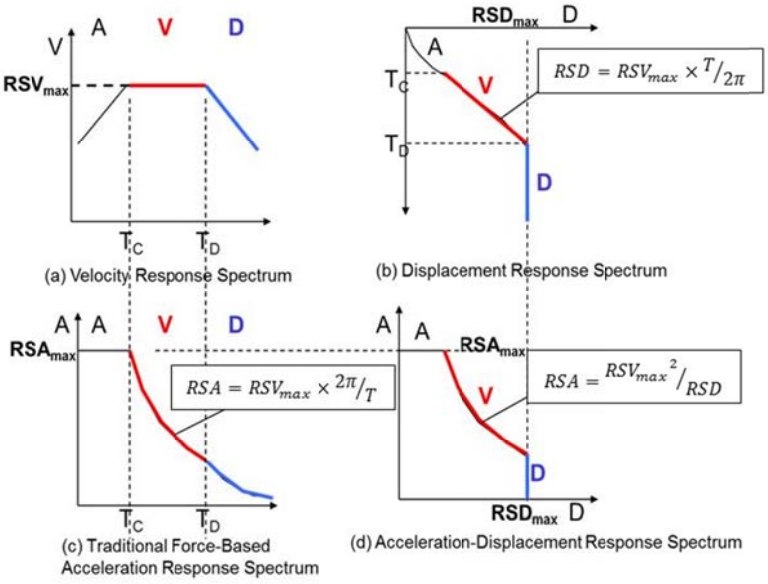

Fig. 3 Response spectrum in four different formats

3. Assessment of Torsionally Balanced Buildings by The *Generalised Force Method*

The example problem used for illustrating the extended lateral force method is based on a nine-storey building which is supported laterally by a frame-wall system (Fig 4(a)) and a design response spectrum (Fig. 4(b)). The fundamental natural period of vibration of the building in seconds was estimated from the empirical expression of Eq. (1) as per clause 4.6 of Eurocode 8 (EN 1998-1 2004)

$$T_1 = 0.05H^{3/4} = 0.05(28)^{3/4} = 0.6\ s \quad \text{where H is height of building in metres} \tag{1a}$$

$$\text{Base shear } F_B = S_D\,\lambda\, m, \tag{1b}$$

where $S_D = 1.9\ m/s^2$, $\lambda = 0.85$ as per clause 4.5 of Eurocode 8.

Assuming that the total seismic mass of the building $m = 410$ t, then

$$F_B = 1.9\ m/s^2 \times 0.85 \times 410\text{t} = \underline{660\text{ kN}}$$

The distribution of seismic forces up the height of the building as shown in Fig. 5 was obtained by applying clause 4.10 of Eurocode 8 which is typical of most seismic codes around the world. The deflection value was obtained by the structural analysis of the wall frame system (details of the computations are not shown as the focus of this article is on how to process the calculated deflection values).

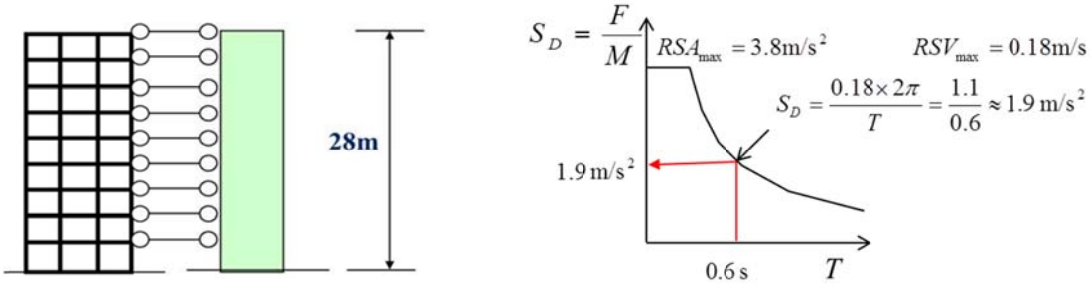

(a) 9 storey frame-wall system (b) loading model

Fig. 4 Example for illustration

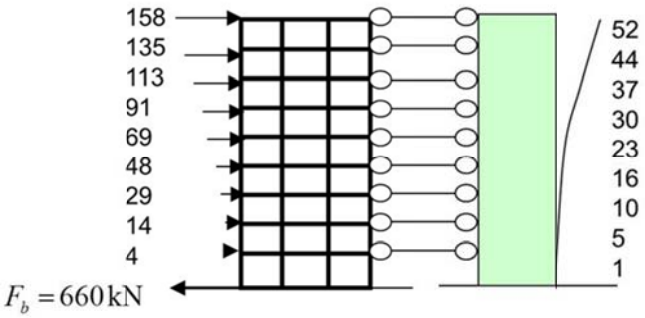

Fig. 5 Results of static analysis showing lateral deflection

The floor displacement values are then processed as shown in Table 1 and then substituted into Eq. (2) for determination of the effective displacement (δ_{eff}) and into Eq. (3) for determination of the effective mass (m_{eff}) assuming a uniform distribution of mass up the height of the building. An introduction to these parameters can be found in Wilson and Lam (2006). Refer Fig. 6 for a summary of the seismic displacement and base shear demand on the building

$$\delta_{eff} = \frac{\sum m_j \delta_j^2}{\sum m_j \delta_j} = \frac{\sum \delta_j^2}{\delta_j} = \frac{7780}{217} \approx 36 \text{ mm} \tag{2}$$

$$m_{eff} = \frac{\left(\sum m_j \delta_j\right)^2}{\sum m_j \delta_j^2} = \frac{m^2 \left(\sum \delta_j\right)^2}{m \sum \delta_j^2} \tag{3}$$

$$m_{eff} = \frac{45.5^2 \times 217^2}{45.5 \times 7780} = 275 \text{ t}; \qquad \text{RSA} = \frac{660 \text{ kN}}{275\ t} = 2.4 \text{ m/s}^2$$

Table 1 Processing of the deflection value of example building

Floor no.	F_i	δ_j(mm)	δ_j^2(mm^2)
1	158	52	2726
2	135	44	2012
3	113	37	1401
4	91	30	900
5	69	23	516
6	48	16	250
7	29	10	93
8	14	5	22
9	4	1	2
SUM	**666**	**217**	**7780**

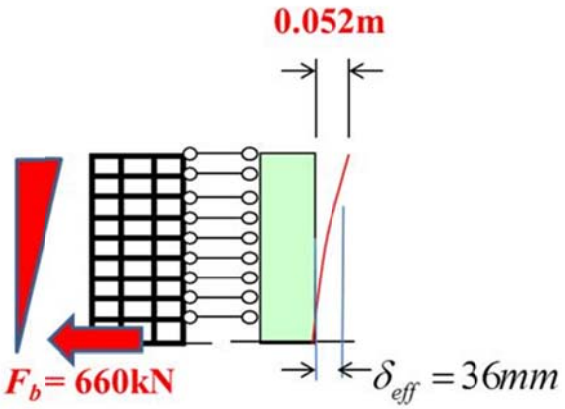

Fig. 6 Calculated displacement

The effective stiffness (k_{eff}) and effective natural period (T_{eff}) of the building are hence obtained using standard expressions as follows:

Effective Stiffness $k_{eff} = \frac{660}{0.036} = 18350$ kN/m

Effective Natural Period $T_{eff} = 2\pi\sqrt{\frac{m_{eff}}{K_{eff}}} = 2\pi\sqrt{\frac{275}{18350}} = 0.77$ s

The diagram showing the stiffness behaviour of the building in the *RSV* vs *RSA* format (also known as the "*capacity diagram*") is then constructed as shown in Fig. 7. Meanwhile, the *ADRS* diagram which was constructed using the expressions shown in Fig. 3 is then overlaid on the *capacity diagram* to identify the effective displacement (δ_{eff}) value of 22 mm (Fig. 8) a roof deflection value of 32 mm and a base shear value of 400 kN (Fig. 9). These refined estimates are considerably less than the initial δ_{eff} estimates of 36 mm, roof displacement of 52 mm and a base shear of 660 kN from the code lateral force method.. The extended lateral force method as described in the above, which is given the name *The Generalised Force Method*, involves calculation of the imposed seismic force and displacement demand on the building in one analysis. The *Generalised Force Method* is distinguished from the existing *Code Lateral Force Method* in that the natural period of vibration of the building need not be pre-determined as is calculated from the analysis procedure based on the given mass and stiffness properties of the building. Both analysis methods are called "Force Method" as they involve applying an array of lateral forces from the side of the building forming part of the calculation procedure.

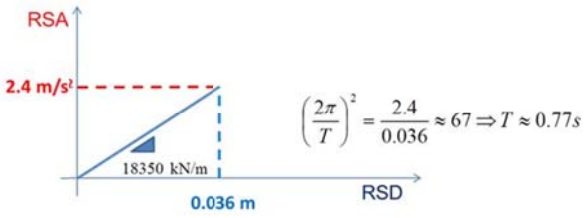

Fig. 7 Effective stiffness and natural period

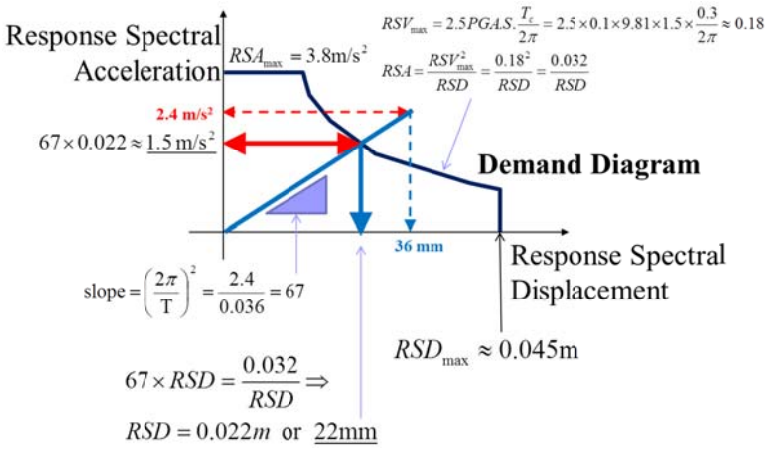

Fig. 8 Seismic displacement and acceleration demand

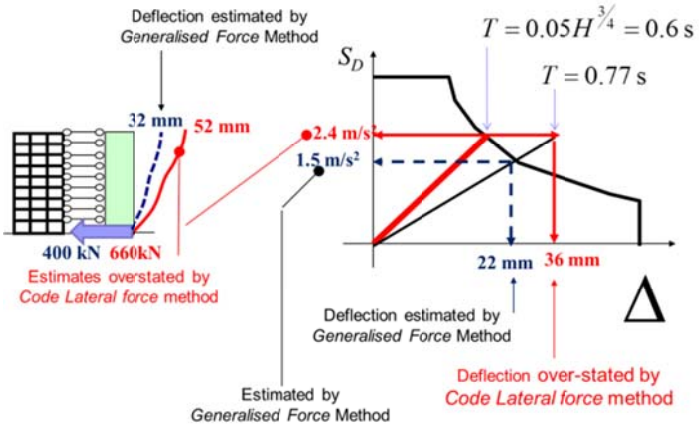

Fig. 9 Comparison of results from the different methods

4. Displacement amplification ratios of torsionally unbalanced buildings

The most comprehensive and detailed literature review by Anagnostopoulos *et al.* (2015) ever undertaken on this topic revealed that some 600 - 700 articles in the past 30 years have been written on the response behaviour of TU structures but many of the findings are contradictory making it difficult to agree definitive design recommendations. These differences between studies stem from different types of models, different definitions of parameters and diversity in the choice of excitations used for input into the torsional analysis studies. Most of the investigations focused on ensuring that the horizontal displacement demand of the individual walls and columns, in the building could be represented by static methods using e_d as the critical design parameter to represent torsional effects. In order to alleviate much of the modelling uncertainties it was advocated by Lee and Hwang (2015) to abolish the long established practice of modelling e_d to account for the complex behaviour of a TU building given that the real time dependent behaviour of the offset of the inertia force was found to be totally inconsistent with current assumptions made in design. An alternative demand model for TU buildings featuring the interaction between shear and torsional demands was proposed (Lee and Hwang 2015).

Seismic design code of practices typically stipulate two approaches for modelling torsional actions in a TU building which has not been factored into results presented in the planar (2D) analysis of the previous section. The first approach is the static method based on the use of equivalent lateral forces which are applied with a design eccentricity (e_d) to calculate the seismic horizontal displacements of the building and the lateral resisting elements. The second approach is based on the use of dynamic analysis of the structure wherein the centre of inertial force on the building floor is offset from the known position of the centre of mass (*CM*) by what is known as the accidental eccentricity (e_a) to take into account uncertainties in the actual location of the *CM*, stiffness properties of the lateral resisting elements and the effects of rotational ground motions. Both approaches put emphasis on the positioning of the applied seismic actions as defined by the value of e_d (Lee and Hwang 2015).

Contemporary code procedures tend to be aligned with the second approach which requires dynamic analysis of the building to be undertaken irrespective of its height. This paper is aimed at developing (an alternative) analysis procedure which waives away the need of a dynamic analysis

for low-medium rise TB and TU buildings.

The simplified assessment method to be presented later in this paper was guided by an alternative modelling strategy which essentially is an extension of the analysis procedure presented for TB buildings in the earlier part of the paper (Section 3). The objective was to capture the trend of increases in the displacement demand of critical elements in the building with the variation in values of the design parameters. To achieve this modelling objective the following steps were undertaken as presented in the later part of this section:

• Justify the adoption of a very simplified form of modelling to be employed for parametric studies for torsional response behaviour (Section 4.1),

• Analyse the frequency behaviour and ratio of translation and rotation associated with the two coupled vibration modes (Section 4.2),

• Derive expressions for the displacement time-histories at the stiff and flexible edges of the floor model in order that the torsional response behaviour can be simulated readily on MATLAB or EXCEL (Section 4.3),

• Identify the maximum displacement demand trends of the two edges for *acceleration*, *velocity* and *displacement* controlled conditions and have the results presented in the form of the displacement ratio (that has been normalised with respect to the displacement of the corresponding TB building (Sections 4.4).

4.1 Single-storey building model and justifications

The nature of the analyses and the choice of the input parameters were based on the following considerations:

(i) The torsional response behaviour of regular TU building models as obtained from 3D analyses were found to be reasonably represented by similar analyses undertaken on suitably chosen simple single-storey models as commented in the literature review by Anagnostopoulos *et al.* (2015). Similar comparative analyses have also been undertaken on a wider form of multi-storey buildings that were supported jointly by structural walls and moment resisting frames (Lam *et al.*1997). It was concluded that the envelope of results obtained from the multi-storey and single story models were generally consistent provided that higher modes effects in the building could be neglected. In view of these observations and the fact that this paper is concerned with buildings of up to 30 m in height (where higher mode effects are less critical) analytical results to be presented in the later part of the paper were derived from simple models comprising only a single-storey floor plate.

(ii) Given that the objective of the analytical investigation was to derive a simplified assessment method to provide estimates of the displacement demand which matches with results from elastic modal analyses (as stipulated by most current codes of practices) building models to be employed for investigations in this study were of linear elastic behaviour. The distinction of a flexible-base model from a fixed-base model was accordingly not as critical. Excitations were represented in the form of a design response spectrum consistent with code procedure as opposed to time-history analyses involving the use of accelerograms.

(iii) The floor plan of building models employed in the investigation had a uni-axial asymmetrical arrangement of lateral resisting elements. Horizontal excitations were applied in a direction which was normal to the axis of symmetry of the building on plan. Building models with uni-axial asymmetry has been shown to be able to provide conservative estimates for the torsional response behaviour of buildings with bi-axial asymmetry (Tsicnias 1981, Stathopoulos and

Anagnostopoulos 2000, 2003).

(iv) Results derived from analyses can be generalised into floor plans of different shapes if dimensions of the floor have been normalised with respect to the mass radius of gyration (r) as opposed to the gross dimensions of the floor.

(v) When deriving the equations of dynamic equilibrium of the torsionally coupled system the origin at which the floor rotates about is considered the *CM* (as opposed to the centre of rigidity *CR*) in order that the *mass* matrix is an identity matrix.

Research undertaken in recent years into analysis methodologies for seismically induced torsional response behaviour of buildings have been based upon non-linear quasi-static (pushover) procedures (e.g., Poursha *et al.* 2014, Cimellaro *et al.* 2014, Bosco *et al.* 2013, Magliulo *et al.* 2012, D'Ambrisi *et al.* 2009). In low seismicity regions, designers typically employ static, or dynamic, analysis procedures assuming linear elastic behaviour of the structural system. Designers working in those environments would be interested in behavioural trends that are consistent with the assumption of linear elasticity. The *Generalised Force Method of Analysis* as presented in this paper are accordingly based on this assumption in order to be in alignment with current design practices in lower seismicity environments.

The single-storey building model (illustrated in Fig. 10) is rectangular in plan with width 2*B* and with the centre of rigidity (CR) offset from the centre of the building by the eccentricity (*e*). Although the modelling was based on a regular building the trends observed are generally applicable to most buildings. Other relevant dynamic and stiffness properties of the building model are as defined by the following parameters:

$M =$ mass; $J =$ torsional moment of inertia; $J = Mr^2$; $r =$ mass radius of gyration

$K_x =$ horizontal stiffness in the xdirection; $K_t =$ torsional stiffness; $\frac{K_t}{K_x} = b^2$

$B = d$istance from the edge of the building to the centre of the floor plate in the direction perpendicular to the direction of excitation.

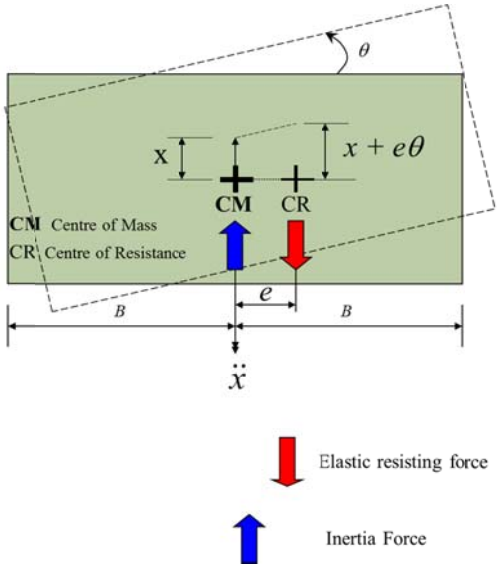

Fig. 10 Schematic diagram showing the generic single-storey floor model

Parameter "*b*" is used to characterise the torsional stiffness properties of the model. The higher the *b* value the higher the torsional stiffness of the lateral supporting elements in relation to their collective translational stiffness (imagine that the simplified model of the building is supported only by a pair of frames then 2*b* is the frame spacing, and *b* is the perpendicular offset of the frame from the *CR* position). Parameter "*B*" which is not to be confused with "*b*" has been defined in the above and in Fig. 10. The value of *B* (as defined above) is 1.25 (for square plate) and can be up to 1.75 (for rectangular floor plate with a very high aspect ratio) times the mass radius of gyration (*r*).

4.2 Frequency and displacement-rotation behaviour of the coupled modes of vibration

A building model featuring uniaxial asymmetry will have every translational mode of vibration resolved into two coupled torsional modes of vibration. Thus, the example (asymmetrical) single-storey building model features two coupled modes of vibration, and not just a single mode, even though the model is a rectangular floor plate. The two coupled modes are increased to three if the model features bi-axial asymmetry (i.e., asymmetry in both directions). The dynamic response behaviour of the structure in natural (free) vibration is not a simple harmonic function (as in the case of a symmetrical single-storey model) but the sum of two harmonics each of which is associated with a coupled torsional mode of vibration. The first mode has a natural angular frequency ($\Omega_{j=1}$) which is lower than that of the corresponding symmetrical building model (ω_x) whereas the second torsional mode of vibration has angular natural frequency ($\Omega_{j=2}$) which is higher than ω_x. Values of the two frequency ratios $\lambda_{j=1,2}$ as defined by Eq. (4) are summarised in Fig. 11

$$\Omega_{j=1,2} = \lambda_{j=1,2} \times \omega_x \tag{4a}$$

where

$$\lambda_j^2 = \frac{1 + (b_r^2 + e_r^2)}{2} \pm \sqrt{\left[\frac{1 - (b_r^2 + e_r^2)}{2}\right]^2 + e_r^2} \tag{4b}$$

It is shown that the value of λ_1 is always smaller than unity whereas the value of λ_2 is always greater than unity. Frequency values of the two coupled modes can be very close (i.e., λ values of both modes are close to unity) when the value of b_r (i.e., *b/r*) is also close to unity, and more so for small eccentricity values. The values of both λ_1 and λ_2 were obtained as solution to an eigenvalue problem forming part of the modal dynamic analysis of the building model the details of which have been illustrated in Appendix A. It is shown that the value of the eccentricity parameter e_r (i.e., *e/r*) can have some effects on the dynamic response behaviour on the building system but its extent of influence depends highly on the value of the other parameter b_r (*b/r*) and the mode of vibration. Another important outcome of the dynamic modal analysis is the shape of deflection of the building in natural vibration. With the analysis for torsional behaviour (of a single-storey building model) the "deflection shape" as obtained from modal analysis is essentially the amount of rotation of the floor plate in the horizontal plane associated with each of the two vibration modes. It was found that the amount of rotation of the building floor is dependent on the value of λ^2 and the offset of the centre of rigidity (*CR*) of the building from the centre of mass (*CM*) as illustrated by the schematic diagrams of Figs. 12(a) and 12(b).

Relationships defining the normalised displacement value at the *CM* and *CR* positions for the

two coupled vibrational modes as illustrated in Figs. 12(a) and 12(b) are as follows

$$\begin{Bmatrix} x_r \\ \theta \end{Bmatrix} = \begin{Bmatrix} 1 \\ \left(\frac{\lambda_j^2 - 1}{e_r}\right) \end{Bmatrix} \tag{5a}$$

where, $x_r = x/r$ and $e_r = e/r$

The vector equality of Eq. (5a) can be re-written into the algebraic expressions as follows

$$\frac{x_{CM}}{r} = 1 \; or \; x_{CM} = r; \qquad x_{CR} = x_{CM} + \theta \times e = r + \left(\frac{\lambda_j^2 - 1}{\frac{e}{r}}\right) \times e = \lambda_j^2 \, r \tag{5b}$$

It can be shown that when the displacement of the building has been normalised with respect to the displacement at its *CM* (i.e., x_{CM}=1) then $x_{CR}=\lambda^2_j$ (as presented diagrammatically in Figs. 12(a) and 12(b)). The high displacement demand at the "stiff" edge of the building (i.e., edge closer to the CR) as shown in Fig. 12(b) may appear counter intuitive to those who base their reasoning on static behaviour. The opposite sense of rotation in the vibrational modes as shown in the figures is reflective of the reversible, and cyclic, nature of dynamic behaviour. In summary, values of λ control frequency behaviour in the coupled vibration modes (Fig. 11) whereas values of λ^2control the amount of rotation in each mode of vibration (Fig. 12).

For those whose mindset are framed by results from static analyses, the offset of the *CR* from the *CM* (i.e., the eccentricity) is the most dominant factor controlling torsional actions. However, this notion is contradicted by the following observations from results of dynamic modal analysis:

(i) The value of λ (and λ_1 in particular) is only weakly dependent on the value of *e/r* as shown by Fig. 11;

(ii) In cases of *b/r* >1 the value of λ_1 for the lower frequency mode of vibration becomes very insensitive to change in the *e*/*r* and *b*/*r* values;

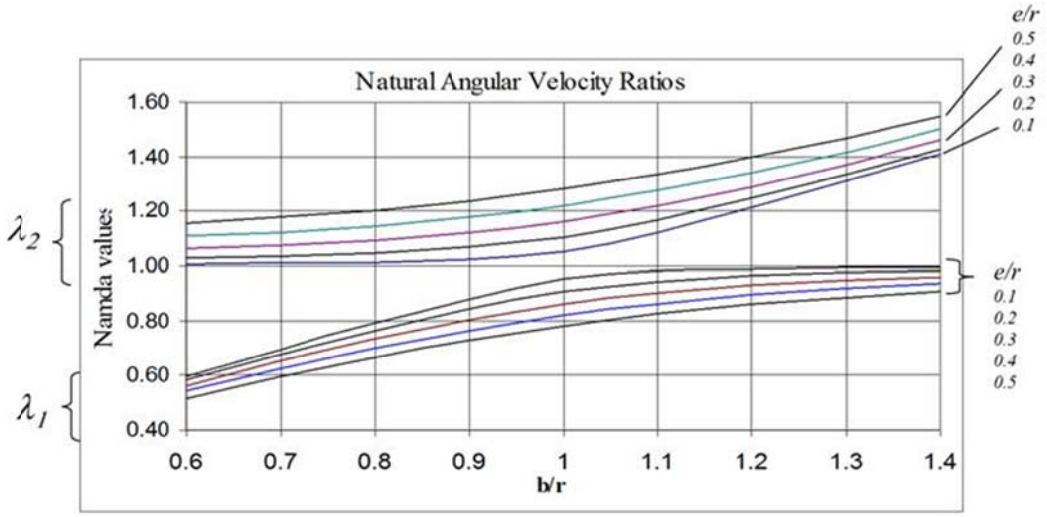

Fig. 11 Frequency ratios of the two coupled vibration modes

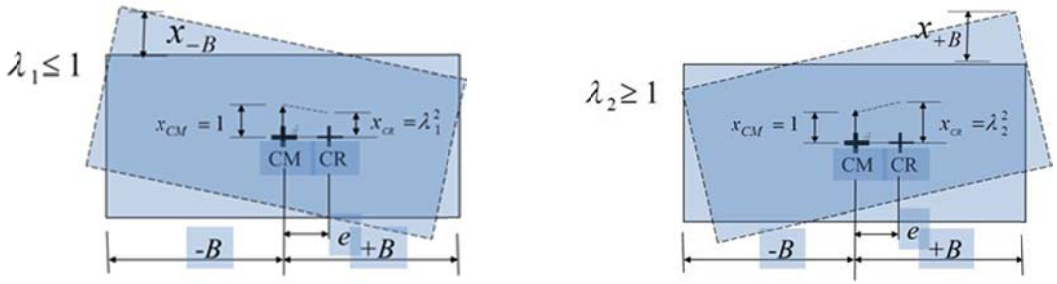

(a) 1st coupled mode of vibration (b) 2nd coupled mode of vibration

Fig. 12 Normalised displacement of the two coupled vibration modes

(iii) For a given value of λ the amount of rotation is actually smaller, and not larger, when the value of the eccentricity is increased (as evident in Fig. 12(a)).

The two vibration modes feature opposite sense of horizontal rotation which is a phenomenon that cannot be replicated by quasi static actions (Figs. 12(a) and 12(b)).

4.3 Expressions for displacement time-histories at the two edges

The displacement time-history at any selected position on the floor plate is the sum of contributions by the two coupled modes of vibration. For each contributing mode the displacement time-history is the product of three factors:

(i) Normalised displacement value at the position of interest;

(ii) Participation factor, *PF* (given by Eq. 7(d));

(iii) Displacement time-history $U_{\Omega,\xi}(t)$ of a single-degree-of-freedom system which has natural angular frequency Ω equal to that of the respective coupled mode of vibration, where ξ is the viscous damping ratio.

In summary, the normalised displacement value is equal to unity at the *CM* position; λ^2at the *CR* position; and $x_{\pm B}$, as defined by Eqs. (6a) and (6b) at the two edges (refer Figs. 12(a) and 12(b))

$$x_{-\mathrm{B}} = 1 + (\lambda_1^2 - 1)\left(\frac{-\mathrm{B}}{e}\right) \text{ where } \lambda_1^2 - 1 \leq 0 \text{ for the 1st mode} \tag{6a}$$

$$x_{+\mathrm{B}} = 1 + (\lambda_2^2 - 1)\left(\frac{+\mathrm{B}}{e}\right) \text{ where } \lambda_2^2 - 1 \geq 0 \text{ for the 2nd mode} \tag{6b}$$

With both expressions a positive value of x_{-B} and x_{+B} will be calculated.

Expressions for determining the time-history of the displacement at the *CM*, *CR* and edges +B and –B are listed in Eqs. (7a) and (7b)

$$\text{At } CM \qquad x_{CM}(t) = \sum_{j=1}^{2} 1 \times PF_j \times U_{\Omega_{j,\xi}}(t) \tag{7a}$$

$$\text{At } CR \qquad x_{CR}(t) = \sum_{j=1}^{2} \lambda_j^2 \times PF_j \times U_{\Omega_{j,\xi}}(t) \tag{7b}$$

Expressions for determining the time-history of the displacement at the at the two edges +B and –B are accordingly listed in Eqs. (7c) and (7d)

$$x_{\pm\mathrm{B}}(t) = \sum_{j=1}^{2}\left(1 + \left(\lambda_j^2 - 1\right)\left(\frac{\pm\mathrm{B}}{e}\right)\right) \times PF_j \times U_{\Omega_{j,\xi}}(t)$$
$$or\ x_{\pm\mathrm{B}}(t) = \sum_{j=1}^{2}\left(1 + \frac{\lambda_j^2 - 1}{e_r}(\pm B_r)\right) \times PF_j \times U_{\Omega_{j,\xi}}(t) \quad (7c)$$

where

$$PF_j = \frac{\begin{Bmatrix}1 & \frac{\lambda_j^2-1}{e_r}\end{Bmatrix}\begin{bmatrix}1 & 0\\ 0 & 1\end{bmatrix}\begin{Bmatrix}1\\ 0\end{Bmatrix}}{\begin{Bmatrix}1 & \frac{\lambda_j^2-1}{e_r}\end{Bmatrix}\begin{bmatrix}1 & 0\\ 0 & 1\end{bmatrix}\begin{Bmatrix}1\\ \frac{\lambda_j^2-1}{e_r}\end{Bmatrix}} = \frac{1}{1+\left(\frac{\lambda_j^2-1}{e_r}\right)^2}, \quad (7d)$$

Eqs. (7a)-(7c) can be re-written into Eqs. 8(a)-8(d)

$$x_{CM}(t) = \sum_{j=1}^{2}\frac{1}{1+\theta_j^2} \times U_{\Omega_{j,\xi}}(t) \quad (8a)$$

$$x_{CR}(t) = \sum_{j=1}^{2}\lambda_j^2\frac{1}{1+\theta_j^2} \times U_{\Omega_{j,\xi}}(t) \quad (8b)$$

$$x_{\pm B}(t) = \sum_{j=1}^{2}\left(1 + \theta_j(\pm B_r)\right) \times \frac{1}{1+\theta_j^2} \times U_{\Omega_{j,\xi}}(t) \quad (8c)$$

where

$$\theta_j = \frac{\lambda_j^2 - 1}{e_r} \quad (8d)$$

A computer program operated on common platforms like EXCEL, or MATLAB, is well capable of simulating the dynamic torsional response behaviour of an asymmetrical building model by the use of Eqs. (7a)-(7d) or Eqs. (8a)-(8d).

4.4 Trends for edge displacements

A response spectrum represents the maximum response of a single-degree-of-freedom system to an earthquake ground motions from time-history analyses. Results from analyses of the TU systems are presented in terms of the displacement ratio (Δ/Δ_o). Δ is the maximum displacement of the TU systems at the edges and Δ_o is the maximum displacement of the equivalent TB systems (TB systems with angular natural frequency equal to the uncoupled angular natural frequency of the TU systems). Δ_o can be represented by the response spectral displacement $RSD(T, \xi)$ where T is the uncoupled natural period of the TU systems.

The displacement ratio (Δ/Δ_o) is expressed as functions of dimensionless parameters e_r (representing offset of the *CM* from the *CR*) and b_r (representing the rigidity of the system in resisting rotation) for *acceleration, velocity*, and *displacement* controlled conditions. The

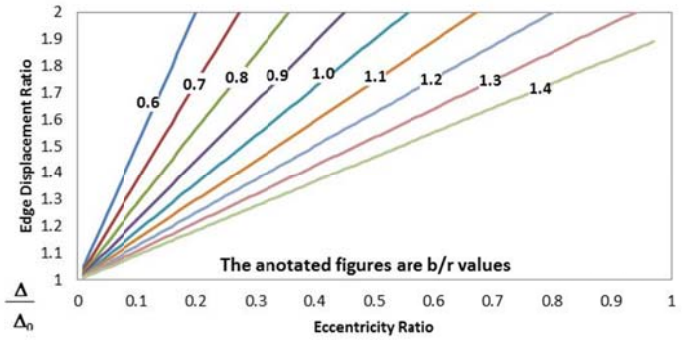

Fig. 13 Edge Displacement Ratios according to results from static analyses (B_r=1.8)

behaviour of the displacement ratios is highly dependent on such conditions and hence results are presented under separate sub-headings for comparison with results based on simply applying a static force at the *CM*. The displacement ratio based on applying a static force at the CM is given by Eq. (9)

$$\frac{\Delta}{\Delta_o} = 1 + \frac{e_r}{b_r^2} B_r \tag{9}$$

The displacement ratio based on Eq. (9) is presented in Fig. 13 assuming B_r=*B/r* of 1.8 to represent a rectangular plan with a very high aspect ratio. These behavioural trends with the edge displacement ratios are shown in Figs. 13, 15, 17 and 19. It is noted that these figures are meant to provide estimates of the maximum displacement at the edges of a TU system that has B_r value close to 1.8. In situations where the value of B_r of the building is different to 1.8 it is recommended to use Eq. (9) which is generally applicable (whilst Fig. 13 only applies to cases where B_r=1.8).

4.4.1 Edge displacement trends in acceleration controlled conditions

The maximum estimated displacement value of a single-degree-of-freedom system ($U_{\Omega j,\xi}$(max)) is represented by the response spectral displacement $RSD(T_j, \xi)$ which is function of natural period of vibration (T_j) and damping ratio (ξ). In the acceleration controlled region of the response spectrum (Fig. 14), the value of response spectral displacement can be taken to be equal to the value defined by Eq. (10)

$$U_{\Omega_{j,\xi}}(\max) = RSD(T_j, \xi) = RSA_{max} \times \left(\frac{T_j}{2\pi}\right)^2 \tag{10}$$

where RSA_{max} is the highest response spectral acceleration demand as defined by the flat part of the design response spectrum.

Substituting Eq. (10) into Eqs. (8a)-(8c) and applying *square-root-of-the-sum-of-the-square* (SRSS) combination rule provides an estimate of the maximum displacement demand at designated positions. Although more rigorous combination rules could be adopted it has been shown that reasonably accurate estimates of the maximum displacement demand can be obtained by employing the simpler *SRSS* combination rule with this form of analysis (Lumantarna *et al.* 2013). Maximum displacement estimates at *CM*, *CR* and at the two edges +B and –B can be determined using the following relationships for comparison with based on simply applying a

static force at CM (Fig. 13)

$$\text{At } CM \qquad \frac{\Delta}{\Delta_0} = \frac{x_{CM}(\max)}{RSD(T,\xi)} = \sqrt{\sum_{j=1}^{2}\left[\frac{1}{1+\theta_j^2}\times\frac{1}{\lambda_j^2}\right]^2} \tag{11a}$$

$$\text{At } CR \qquad \frac{\Delta}{\Delta_0} = \frac{x_{CR}(\max)}{RSD(T,\xi)} = \sqrt{\sum_{j=1}^{2}\left[\frac{\lambda_j^2}{1+\theta_j^2}\times\frac{1}{\lambda_j^2}\right]^2} \tag{11b}$$

At the two edges which are offset by the amount +B and –B from the CM

$$\frac{\Delta}{\Delta_0} = \frac{x_{\pm B}(\max)}{RSD(T,\xi)} = \sqrt{\sum_{j=1}^{2}\left[\frac{1+\theta_j(\pm B_r)}{1+\theta_j^2}\times\frac{1}{\lambda_j^2}\right]^2} \tag{11c}$$

Figs. 15(a) and 15(b) present two sets of estimates of the edge displacement ratio $\frac{x_{\pm B}(\max)}{RSD(T,\xi)}$ or Δ/Δ_o as obtained using Eq. (11c) for the two edges assuming that B_r (=B/r) is equal to 1.8. One of the edges is on the far side of the *CR* (the "flexible side") and the other edge is on the near side of *CR* (the "stiff side"). It is shown in Figs. 15(a) and 15(b) that the displacement at the stiff and flexible edges of the *TU* building is highly dependent on the value of *b/r* representing the torsional rigidity of the building which is shown to be much more influential to torsional coupling behaviour than the eccentricity properties.

TU models with values of *b/r* lower than unity are shown to have the displacement ratio Δ/Δ_o reaching a very high value. Graphs associated with $b/r \leq 1.0$ are accordingly shown in dotted lines to indicate that such conditions should be prohibited in the design of a building irrespective of whether *lateral force method* or *dynamic analysis method* has been employed for analysis in view of high displacement demand, and counter intuitive, behaviour in such conditions as shown in Fig. 15(a). Codes of practices (e.g., Eurocode 8 (EN 1998-1 2004) encourage the use of orthogonal elements for providing adequate torsional rigidity to the building and classify buildings in which $b/r \leq 1.0$ as irregular. Graphs in solid lines which are associated with higher *b/r* values ($b/r > 1.0$) show a gradual, monotonic, increase in displacement demand with increasing eccentricity. However, the trends are still very different to statical behaviour as shown in Fig. 13.

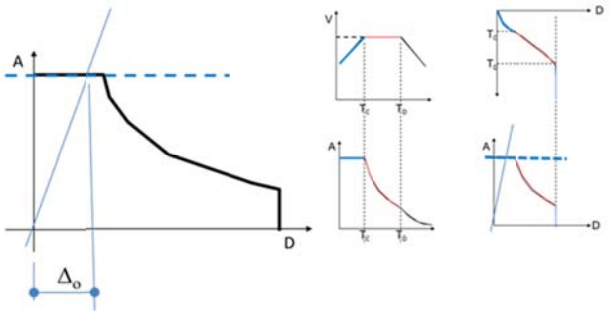

Fig. 14 Acceleration controlled conditions

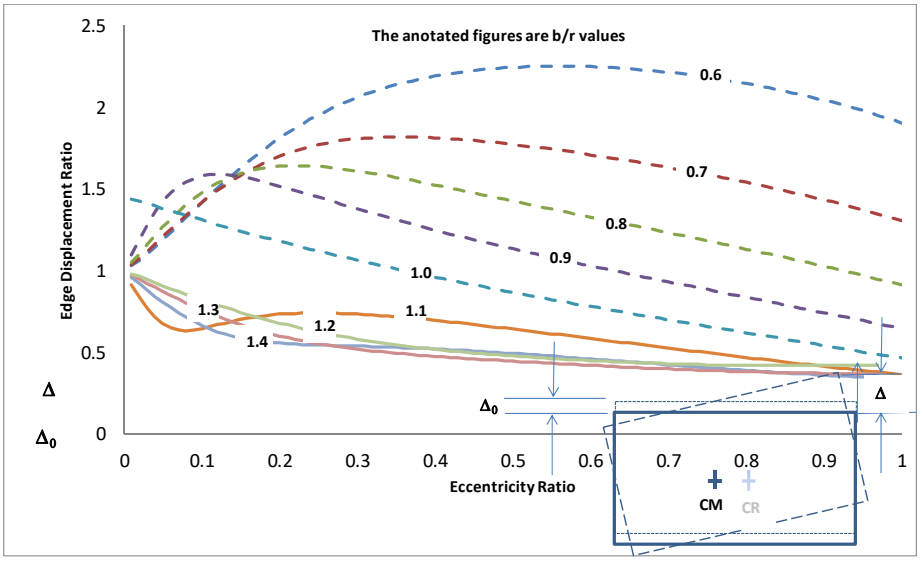

(a) Stiff edge

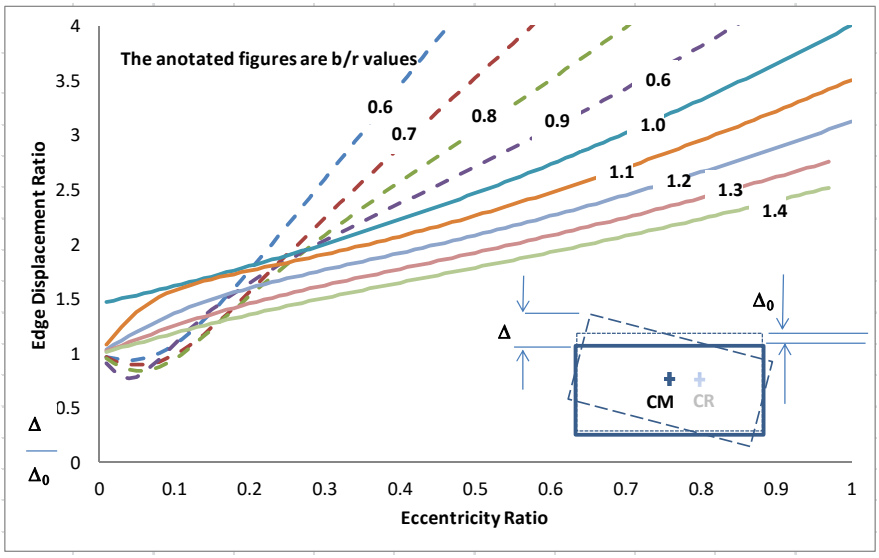

(b) Flexible edge

Fig. 15 Displacement ratio of TU buildings in acceleration controlled conditions (B_r=1.8)

Figs. 15(a) and 15(b) may be used for finding the value of the displacement ratio Δ/Δ_o where value of B_r is close to 1.8. In situations where the value of B_r is very different to 1.8 it is recommended to use Eq. (8d) to calculate the value of θ_j, and then Eq. (11c) to calculate the value of Δ/Δ_o.

4.4.2 Trends of edge displacement in velocity controlled conditions

In the velocity controlled region of the response spectrum (Fig. 16), the value of response spectral displacement may be estimated using Eq. (12)

$$U_{\Omega_{j,\xi}}(\max) = RSD(T_j, \xi) = RSV_{max} \times \frac{T_j}{2\pi} \tag{12}$$

Estimates of the edge displacement ratio $\frac{x_{\pm B}(\max)}{RSD(T,\xi)}$ as obtained using Eq. (13c) for the two edges are presented in Figs. 17(a) and 17(b). Graphs in solid lines which are associated with higher b/r values (i.e., b/r>1.0) show a very gradual increase in the ratio Δ/Δ_o with increasing eccentricity. However, with b/r<1.0 counter intuitive behaviour of displacement at the stiff edge of the building can be seen as for acceleration controlled behaviour

$$\text{At } CM \qquad \frac{\Delta}{\Delta_0} = \frac{x_{CM}(\max)}{RSD(T,\xi)} = \sqrt{\sum_{j=1}^{2}\left[\frac{1}{1+\theta_j^2} \times \frac{1}{\lambda_j}\right]^2} \tag{13a}$$

$$\text{At } CR \qquad \frac{\Delta}{\Delta_0} = \frac{x_{CR}(\max)}{RSD(T,\xi)} = \sqrt{\sum_{j=1}^{2}\left[\frac{\lambda_j^2}{1+\theta_j^2} \times \frac{1}{\lambda_j}\right]^2} \tag{13b}$$

At the two edges which are offset by the amount +B and –B from the CM

$$\frac{\Delta}{\Delta_0} = \frac{x_{\pm B}(\max)}{RSD(T,\xi)} = \sqrt{\sum_{j=1}^{2}\left[\frac{1+\theta_j(\pm B_r)}{1+\theta_j^2} \times \frac{1}{\lambda_j}\right]^2} \tag{13c}$$

In view of the trends displayed it is strongly recommended that the torsional rigidity of the building should be greater than the limit corresponding to the value of b/r equal to unity to avoid the erratic behaviour leading to excessive displacement demand of the building that can result as in the case of acceleration controlled behaviour.

Figs. 17(a) and 17(b) may be used for finding the value of the displacement ratio Δ/Δ_o where value of B_r is close to 1.8. In situations where the value of B_r is very different to 1.8 it is recommended to use Eq. (8d) to calculate the value of θ_j, and then Eq. (13c) to calculate the value of Δ/Δ_o.

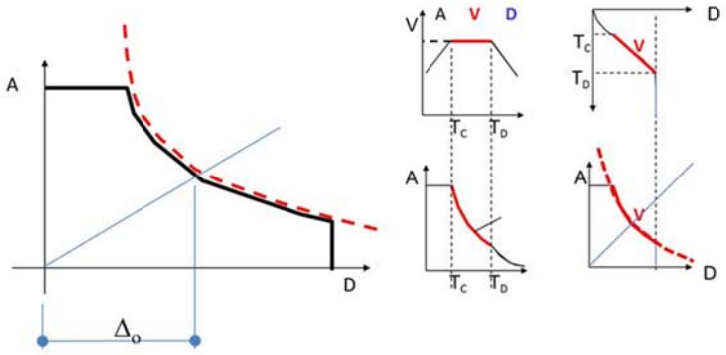

Fig. 16 Velocity controlled conditions

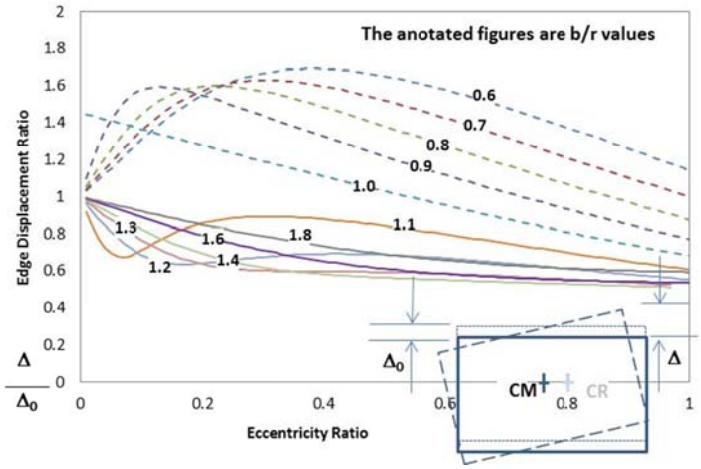

(a) Stiff edge

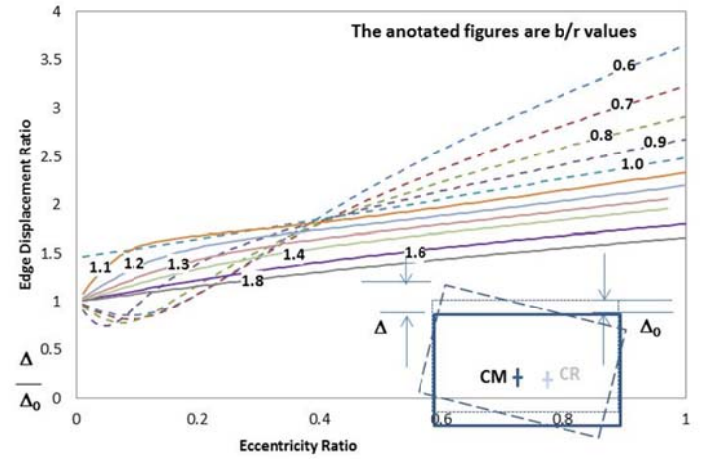

(b) Flexible edge

Fig. 17 Displacement ratio of TU buildings in velocity controlled conditions (B_r=1.8)

4.4.3 Trends of edge displacement in displacement controlled conditions

Finally, in displacement controlled conditions typical of high rise buildings (Fig. 18) the value of response spectral displacement may simply be taken as constant, being the highest displacement demand $RSD_{\max}$ as represented by the flat part of the displacement spectrum of Fig. 2(c). The relationship is defined by Eq. (14)

$$U_{\Omega_{j,\xi}}(\max) = RSD_{max} \tag{14}$$

Buildings up to the height limit of 30 m are expected not to have a natural period of vibration as high as that to be placed in the displacement controlled zone of the response spectrum. However, displacement controlled conditions may be applied for the near collapse assessment of structures as demonstrated in Lumantarna *et al.* (2010, 2013) and Kafle *et al.* (2011), and buildings with a soft-storey in particular (Kafle *et al.* 2015). This is because of the increase in the effective period of vibration caused by inelastic softening of the building in such conditions. Eqs. (13a)-

(13c) are accordingly revised into Eqs. (15a)-(15c) for displacement controlled conditions. Maximum displacement estimates at *CM*, *CR* and at the two edges +B and –B are accordingly given by the following expressions

$$\text{At } CM \qquad \frac{\Delta}{\Delta_0} = \frac{x_{CM}(\max)}{RSD(T,\xi)} = \sqrt{\sum_{j=1}^{2}\left[\frac{1}{1+\theta_j^2}\right]^2} \tag{15a}$$

$$\text{At } CR \qquad \frac{\Delta}{\Delta_0} = \frac{x_{CR}(\max)}{RSD(T,\xi)} = \sqrt{\sum_{j=1}^{2}\left[\frac{\lambda_j^2}{1+\theta_j^2}\right]^2} \tag{15b}$$

At the two edges which are offset by the amount +B and –B from the CM

$$\frac{\Delta}{\Delta_0} = \frac{x_{\pm B}(\max)}{RSD(T,\xi)} = \sqrt{\sum_{j=1}^{2}\left[\frac{1+\theta_j(\pm B_r)}{1+\theta_j^2}\right]^2} \tag{15c}$$

Estimates for the displacement ratio $\frac{x_{\pm B}(\max)}{RSD(T,\xi)}$ or Δ/Δ_o as obtained using Eq. (15c) for the two edges are shown in Fig. 19(a) and 19(b). It is shown that the displacement demands of the building at the edges are acceptable irrespective of the torsional rigidity properties (i.e., *b*/*r* values). Eccentricity is not linearly correlated with the displacement demand, and the displacement ratio Δ/Δ_o is shown to asymptote to an upper limit of 1.6 which is a trend not seen from results of analysis for AC, or VC, conditions. Although it is rare of buildings below 30 m in height to experience DC conditions, results obtained from the use of Eq. (15c) along with the conservative assumption of RSD=$RSD_{\max}$ can be taken as upper bound estimates for the edge displacement of the building irrespective of the conditions of excitations (refer Fig. 2(c)).

Fig. 19(a) and 19(b) may be used for finding the value of the displacement ratio Δ/Δ_o where value of B_r is close to 1.8. In situations where the value of B_r is very different to 1.8 it is recommended to use Eq. (8d) to calculate the value of θ_j, and then Eq. (15c) to calculate the value of Δ/Δ_o.

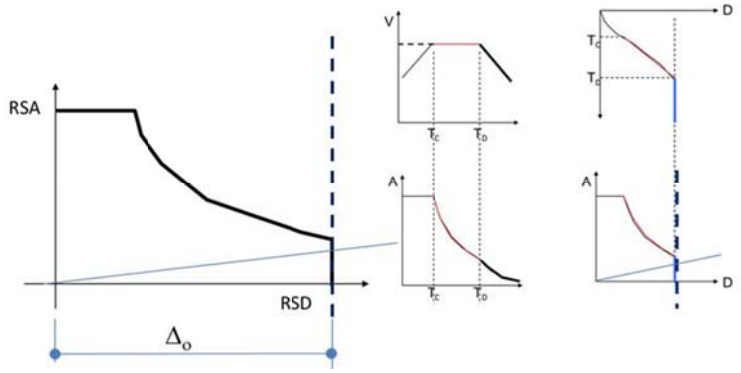

Fig. 18 Displacement controlled conditions

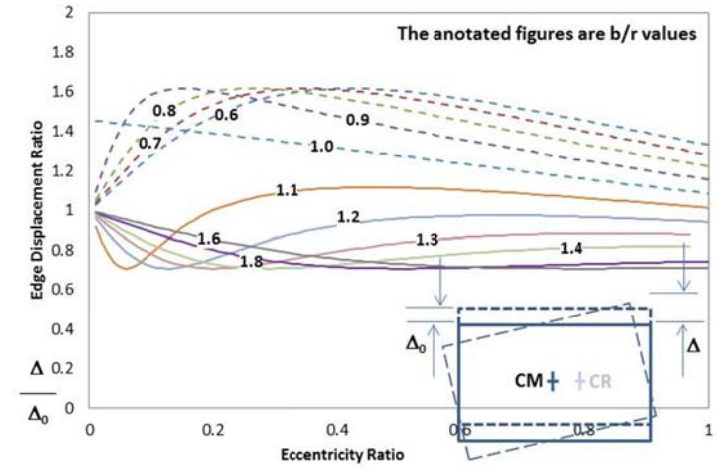

(a) Stiff edge

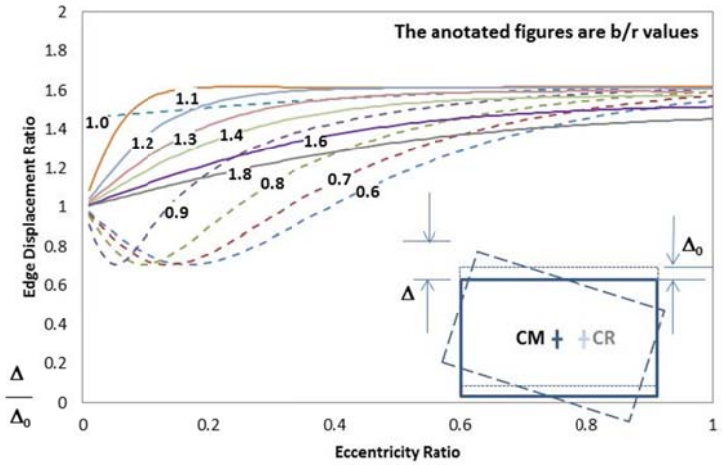

(b) Flexible edge

Fig. 19 Displacement ratio of TU buildings in displacement controlled condition (B_r=1.8)

4.5 Bi-directional excitations

Results presented in the foregoing were based on the response of the building to uni-lateral excitations. It is noted that codes of practices require analyses to be undertaken along the two orthogonal axes and their resultant displacement demand values be combined using the standard (SRSS) combination rule provided that the natural period of vibration in the orthogonal directions are well separated. Alternatively, the element displacement demand resulted from full intensity (100%) excitations applied in one direction is to be combined (by arithmetic summation) to that resulted from 30% excitations applied in the orthogonal direction. Thus, the combined maximum displacement demand of elements in the building in DC conditions would be within 2.1 (i.e., 1.6+0.3×1.6) times the maximum displacement demand calculated from one of the two orthogonal planar models of the building, whichever is the larger.

5. Verification of results from *Generalised Force Method* by comparison with results from dynamic analyses

5.1 Introduction to the case study example building used for the verification study

Three-dimensional dynamic analyses have been performed on a number of multi-storey building models by the authors to verify predictions based on the recommended methodologies presented in Sections 3 and 4. Results of dynamic analyses of an example eight-storey tall reinforced concrete building using program ETABS (Computer & Structures Inc. 2013) are presented in the following. The building was laterally supported by moment resisting frames and reinforced concrete shear walls. Some of the columns in the moment resisting frames were discontinuous at the 1st to 4th level, resulting in vertical irregularities in the building. The plan view at various levels of the building and the 3-D model of the building are presented in Figs. 20 and 21, respectively. The geometric and material properties of the elements of the building are summarised in Table 2. The building model chosen for the verification analysis was derived from a real building that has been analysed and validated by comparison with field measurements by Sofi *et al.* (2013). The height of the building was 28 m and the mass radius of gyration (r) was 18 m. The mass, storey eccentricity and b values of the individual floors have been identified and the normalised values are listed in Table 3 (the normalisation was with respect to the value of r).

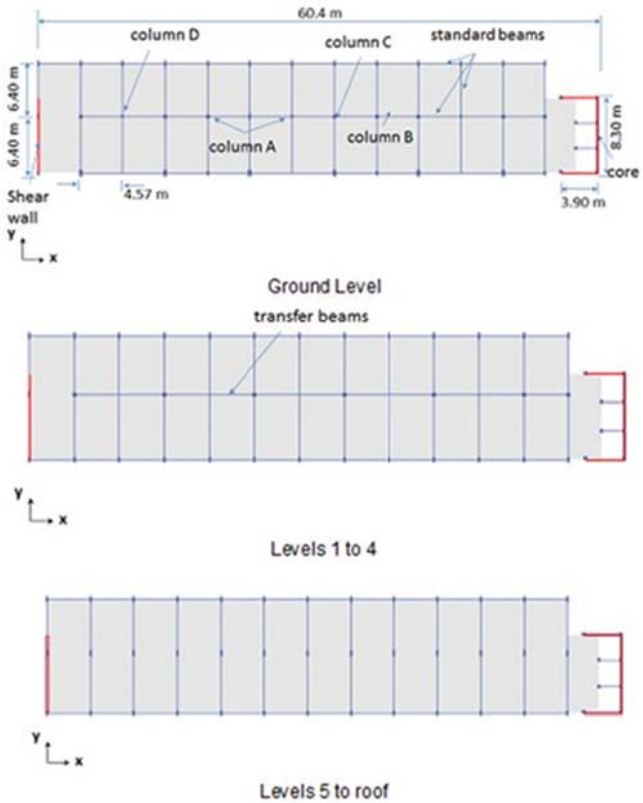

Fig. 20 Plan views of building

5.2 Dynamic modal analyses

Dynamic modal analyses of the building were conducted by employing the design response spectrum of Fig. 4(b). Only the response of the building in the *y*-direction of motion is presented herein given the lower eccentricity values in the orthogonal direction. The fundamental translational natural period of vibration of the planar model of the building in the *y*-direction was 0.7 s and the corresponding torsional coupled periods of the building in the *y*-direction were 0.80 and 0.55 s. Velocity controlled conditions apply in view of the natural period value of the building.

The translational displacement profile of the building from planar (translational only) analysis can be compared with profiles at the flexible and stiff edges as obtained from 3D analyses of the TU model (Fig. 22). The displacement profile at the two critical edges is shown to be similar in shape to that from translational only analysis in spite of irregularities in the building.

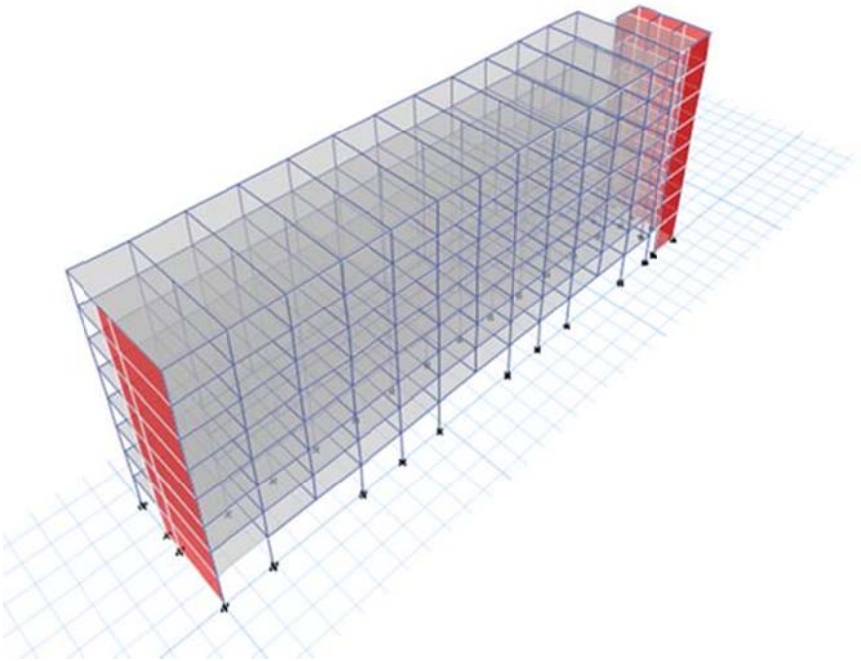

Fig. 21 3-D model of the building

Table 2 Dimensions of principal structural elements and material properties (mm)

Element	**Slab**	**Walls**		**Beams**		**Columns**			
Type		Core	Shear	Standard	Transfer	A	B	C	D
Material	RC*	RC*	RC	RC	RC	RC	RC	RC	RC
Width (mm)	-	200	200	280	280	375	280	400	300
Depth (mm)	250	-	-	620	1000	810	610	400	300
Length (mm)	-			-	-				

*RC - reinforced concrete with modulus of elasticity of 24.5 GPa and density of 2500 kg/m^3

Table 3 Storey mass, eccentricity and torsional stiffness of the building

Level	Storey mass (t)	Eccentricity e_r		Torsional stiffness b_r
		x-direction	y-direction	
1	755	-0.07	0.14	1.50
2	738	-0.02	0.31	1.45
3	738	0.02	0.44	1.40
4	751	0.06	0.53	1.35
5	719	0.08	0.60	1.40
6	719	0.10	0.64	1.50
7	728	0.11	0.67	1.70
8	684	0.12	0.70	1.90

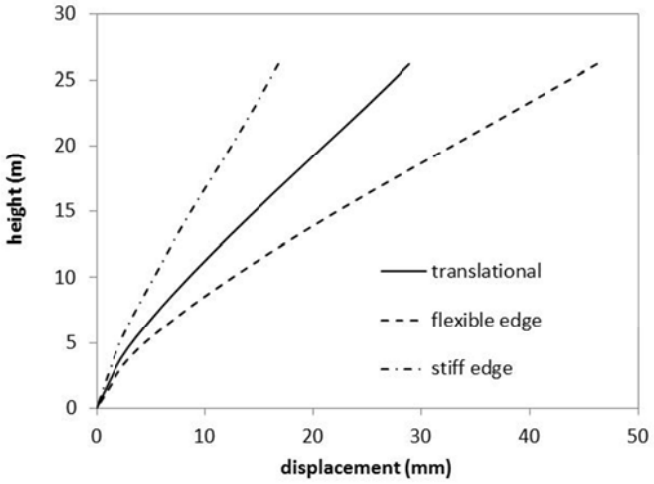

Fig. 22 Displacement profiles from dynamic analyses

5.3 Application of Generalised Force Method as recommended in this paper

The *Generalised Force Method* as outlined in Sections 3 and 4 was applied to obtain estimates of the displacement demand of the example torsionally unbalanced building. The planar analysis method as presented in Section 3 was first performed ignoring on-plan asymmetry of the building. The fundamental natural period of vibration of the building obtained from Eq. (1) was found to be 0.6 s approximately, and the base shear was 9730 kN. The displacement values obtained by applying the base shear distributed up the height of the building in accordance with clause 4.10 of Eurocode 8 (EN 1998-1, 2004) have been digitised and listed in Table 4.

The effective displacement $\delta_{eff} = 31$ mm; effective mass $m_{eff} = 4244$ t;

Effective stiffness $K_{eff} = 355824$ MN/m; Effective natural period $T_{eff} = 0.7$ s

Calculation of these parameter values assuming Torsionally Balanced (TB) conditions based on the storey mass (as listed in Table 3) and the 2D displacement profile (as listed in Table 4) is shown in

Table 4 Displacement values of TB estimated using the *Code Lateral Force Method*

Level	Δ_o (mm)
8	45
7	39
6	32.7
5	26.1
4	19.6
3	13.3
2	7.7
1	3.2

Table 5 Displacement values of TB estimated by the *Generalised Force Method*

Level	Δ_o (mm)
8	34
7	29
6	24
5	20
4	15
3	10
2	6
1	2

Table 6 Displacement values estimated using the Generalised Force Method

Level	**Δ_O (mm)** ***by Generalised Force method*** **(TB)**	**Δ (mm)** ***by Generalised Force Method*** **(TU)**	
		Flexible edge **(×1.73)**	***Stiff edge*** **(×0.55)**
8	34	59	19
7	29	51	16
6	24	43	13
5	20	34	11
4	15	26	8
3	10	17	5
2	6	10	3
1	2	4	1

details in Appendix B. The displacement demand estimated by the *Generalised Force Method* (as outlined in Section 3) is 24 mm based on planar analysis of the building ignoring plan asymmetry. The building displacement profile is represented by the listed values in Table 5.

The displacement demand values of the torsionally unbalanced building were estimated by applying the respective displacement amplification ratios. In summary, the calculation involves the use of Eq. (4b) or Fig. 11 for finding the value of λ_1 and λ_2, Eq. (8d) for finding the value of θ_1 and θ_2, and Eq. (13c) for finding the value of Δ/Δ_o. Given the values of Δ_o that are listed in Table 5 the displacement Δ at the two edges of the TU building can be calculated (Table 6). In this case study to illustrate the method e_r=0.65 and b_r=1.35 (refer Appendix B for details of how those values can be obtained for a building with different floor plans up the height. Applying the method as described the displacement ratio (Δ/Δ_o) is accordingly 1.73 at the flexible edge and 0.55 at the stiff edge of the building. These displacement values of the individual floor are listed in Table 6. Results so obtained are then compared with results from dynamic analyses for verification purposes (Figs. 23(a) and 23(b)). All the steps of the method is summarised in Table 7.

Table 7 Listing of the steps in the *Generalised Force Method of Analysis*

Steps	Descriptions
1	Undertake planar analysis of the building assuming TB conditions to determine the values of Δ_o.
2	Identify the eccentric and torsional stiffness properties of the lateral resisting elements, and the mass radius of gyration of the floors. In situations where those lateral resisting elements vary significantly from floor to floor employ the techniques presented in Appendix C to determine those properties.
3	Use Eq. (4b) or Fig. 11 to determine the values of λ_1 and λ_2
4	Use Eq. 8(d) to determine the values of θ_1 and θ_2
5	Use the following equations to determine the value of Δ/Δ_o: Eq. (11c) for *acceleration controlled* conditions (or Figs. 15(a) and 15(b) if the value of B_r is close to 1.8) Eq. (13c) for *velocity controlled* conditions (or Figs. 17(a) and 17(b) if the value of B_r is close to 1.8) Eq. (15c) for *displacement controlled* conditions (or Figs. 19(a) and 19(b) if thevalue of B_r is close to 1.8)
6	Combine the results from step (1) and Step (5) to determine the value of Δ at both edges of the building.

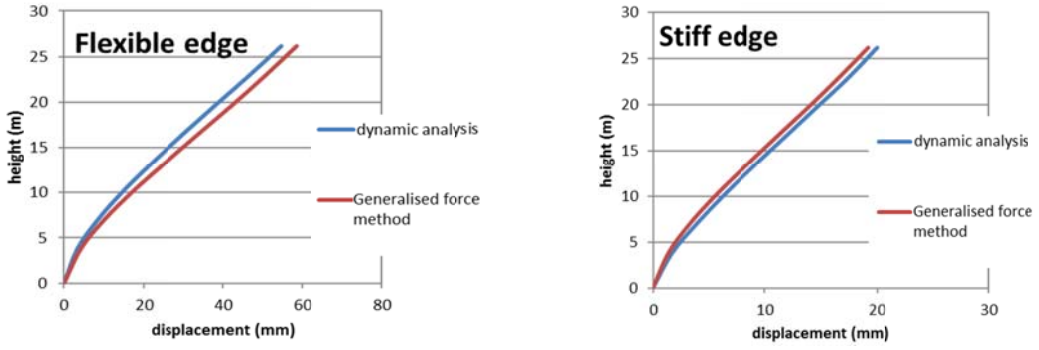

(a) Flexible edge (b) Stiff edge

Fig. 23 Comparison with displacement estimates using the simplified assessment methods

6. Conclusions

The *Generalised Force Method of Analysis* for undertaking design checks for both TB and TU low and medium rise buildings has been derived, and verified, in this paper.

In the proposed procedure a TB building is first subject to the code lateral force analysis method for obtaining an initial estimate of the seismic inertia forces. The code procedure has been extended by the analysis of the deflection profile of the building and in identifying the *effective displacement*, *effective stiffness* and *effective mass* in order that a relationship representing the behaviour of the building can be constructed in the form of a capacity diagram. The response spectrum of the earthquake actions was then presented in the format of an *acceleration-displacement response spectrum* (ADRS) diagram which was overlaid onto the capacity diagram. The displacement and acceleration demand of the building was then taken as the intercept of the capacity diagram with the ADRS diagram. It is shown that the (more accurate) estimate of the seismic demand as indicated by the intercept of the two diagrams was much less conservative than the initial estimate as stipulated by the *code lateral force method*. The method of analysis as introduced herein is called the *Generalised Force Method*.

For a TU building the torsional rigidity parameter (b/r) and eccentricity parameter (e/r) are to be identified. TU buildings with weak torsional rigidity (i.e., $b/r \leq 1.0$) should be prohibited from design irrespective of results from dynamic analyses unless performance is satisfactory under DC conditions. The displacement demand of a medium rise *TU* building in which $b/r \geq 1.0$ may be derived from planar analysis as per the procedure introduced in Section 3. The displacement profile so obtained from the translational only analysis has to be amplified by a factor which is defined by:

(i) Eq. (11c) or Figs. 15(a) and 15(b) for acceleration controlled conditions

(ii) Eq. (13c) or Figs. 17(a) and 17(b) for velocity controlled conditions

(iii) Eq. (15c) or Figs. 19(a) and 19(b) for displacement controlled conditions

Refer Table 7 for a summary of all the steps involved in the analysis method.

The effects of bi-directional excitations would also need to be taken into account by the use of the 100%/30% rule or SRSS combination rule.

The recommended *Generalised Force Method* for estimating the displacement profile of a TU building has been verified by comparison with results from the dynamic analyses of irregular building models. Such verification analysis undertaken for an example building is presented.

Acknowledgments

Financial support from the Australian Research Council (ARC) Discovery Project DP140103350 entitled *Collapse Assessment of Reinforced Concrete Buildings in Regions of Lower Seismicity* is gratefully acknowledged. Contributions made by *Daniel Looi* and *Ir Adjunct Professor MC Hee* in related collaborative work are gratefully acknowledged.

The support of the Commonwealth of Australia through the Cooperative Research Centre program is acknowledged.

References

Abrahamson, N., Silva, W.J. and Kamai, R. (2014), “Summary of the ASK14 ground motion relation for

active Crustal regions", *Earthq. Spectra*, **30**(3), 1025-1055.
Anagnostopoulos, S.A., Kyrkos, M.T. and Stathopoulos, K.G. (2015) "Earthquake induced torsion in buildings: critical review and state of the art", *Earthq. Struct.*, **8**(2), 305-377.
Bosco, M., Ghersi, A. and Marino, E.M. (2013) "Comparison of nonlinear static methods for the assessment of asymmetric buildings", *Bull. Earthq. Eng*., **11**(6), 2287-2308.
Boore, D.M., Stewart, J.P., Seyhan, E. and Atkinson, G.M. (2014), "NGA-West2 equations for predicting PGA, PGV, and 5% damped PSA for shallow crustal earthquakes", *Earthq. Spectra*, **30**(3), 1057-1085.
Campbell, K.W. and Bozorgnia, Y. (2014), "NGA-West2 Ground Motion Model for the average horizontal components of PGA, PGV, and 5% damped linear acceleration response spectra", *Earthq. Spectra*, **30**(3), 1087-1115.
Chiou, B.S.J. and Youngs, R.R. (2014), "Update of the Chiou and Youngs NGA model for the average horizontal component of peak ground motion and response spectra", *Earthq. Spectra*, **30**(3), 1117-1153.
Computers & Structures Inc. (2013), *User's Guide ETABS 2013: Integrated Building Design Software*, Computers & Structures, Inc, Berkeley, California, USA.
Cimellaro, G.P., Giovine, T. and Lopez-Garcia, D. (2014), "Bi-directional pushover analysis of irregular structures", *J. Struct. Eng*., **140**(9), 04014059.
D'Ambrisi, A., De Stefano, M. and Tanganelli, M. (2009) "Use of pushover analysis for predicting seismic response of irregular buildings: A case study", *J. Earthq. Eng*., **13**(8), 1089-1100.
EN 1998-1 (2004), Eurocode 8: Design of Structures for Earthquake Resistance - Part 1: General Rules, Seismic Actions and Rules for Buildings, BSI.
Kafle, B., Lam, N., Gad, E.F. and Wilson, J. (2011), "Displacement controlled rocking behaviour of rigid objects", *Earthq. Eng. Struct. Dyn*., **40**(15), 1653-1669.
Lam, N.T.K. and Wilson, J.L. (2004), "Displacement modelling of intraplate earthquakes", *ISET J. Earthq. Technol.*, **1**, 15-52
Lam, N.T.K., Wilson, J.L. and Hutchinson, G.L. (1997), "Review of the torsional coupling of asymmetrical wall-frame building", *Eng. Struct.*, **19**(3), 233-246.
Lee, H.S. and Hwang, K.R. (2015), "A new nethodology in seismic torsion design of building structures", *Proceedings of the ASEM'15 conference*, August, Seoul.
Lumantarna, E., Lam, N. and Wilson, J. (2013), "Displacement-controlled behavior of asymmetrical single-story building models", *J. Earthq. Eng*., **17**(6), 902-917.
Lumantarna, E., Lam, N., Wilson, J. and Griffith, M. (2010), "Inelastic displacement demand of strength-degraded structures", *J. Earthq. Eng.*, **14**(4), 487-511.
Magliulo, G., Maddaloni, G. and Cosenza, E. (2012), "Extension of N2 method to plan irregular buildings considering accidental eccentricity", *Soil Dyn. Earthq. Eng.*, **43**, 69-84.
PEER (2015), *NGA-East: median ground-motion models for the Central and Eastern North America Region, PEER Report No. 2015/04*, Pacific Earthquake Engineering Research Center, University of California, Berkeley.
Poursha, M., Khoshnoudian, F. and Moghadam, A.S. (2014), "The extended consecutive modal pushover procedure for estimating the seismic demands of two-way unsymmetric-plan tall buildings under influence of two horizontal components of ground motions", *Soil Dyn. Earthq. Eng*., **63**, 162-173.
Standards Australia (2007), *AS 1170.4-2007 Structural Design Actions, Part 4: Earthquake Actions in Australia*, Standards Australia, Sydney, Australia.
Standards New Zealand (2004), *NZS 1170.5 Structural Design Actions, Part 5: Earthquake Actions-New Zealand*, Standards New Zealand, Wellington, New Zealand.
Stathopoulos, K.G. and Anagnostopoulos, S.A. (2000), "Inelastic earthquake response of buildings subjected to torsion", *Proceedings of the 12th World Conference on Earthquake Engineering*, Auckland, February.
Stathopoulos, K.G. and Anagnostopoulos, S.A. (2003), "Inelastic earthquake response of single-story Earthquake induced torsion in buildings: critical review and state of the art asymmetric buildings: an assessment of simplified shear-beam models", *Earthq. Eng. Struct. Dyn*., **32**, 1813-1831.
Sofi, M., Lumantarna, E., Helal, J., Letheby, M., Rezapour, M., Duffield, C.F. and Hutchinson, G.L. (2013), "The effects of building parameters on seismic inter-storey drifts of tall buildings", *Proceedings of the*

2013 Australian Earthquake Engineering Society Conference. *Australian Earthquake Engineering Society Conference (AEES)*, Tasmania, November.

Tsicnias, T.G. (1981), "Coupled lateral and torsional earthquake response of buildings with rigid floor diaphragms", Ph.D Thesis, University of London.

Wilson, J. and Lam, N. (2006), "Earthquake design of buildings in Australia by velocity and displacement principles", *Aust. J. Struct. Eng.*, **6**(2), 103-118.

CC

Appendix A

Dynamic equations of equilibrium and eigenvalue analysis

For completeness this section presents details of how the eigenvalues (λ_j) and eigenvectors (normalised displacement x_r and θ) as presented in the earlier sections of the paper were derived.

Equation of translational equilibrium

$$M\ddot{x} + K(x + e\theta) = 0 \tag{A1a}$$

Equation of rotational equilibrium (taking moment about CM)

$$J\ddot{\theta} + K(x + e\theta)e + K_t\theta = 0 \tag{A1b}$$

Equation of translational equilibrium

$$M\ddot{x} + K_x(x + e\theta) = 0 \tag{A2a}$$

Divide both sides of equation by M and r

$$\frac{\ddot{x}}{r} + \omega_x^2\left(\frac{x}{r} + \frac{e}{r}\theta\right) = 0 \tag{A2b}$$

Given that $\ddot{x_r} = \frac{\ddot{x}}{r}; x_r = \frac{x}{r};\ e_r = \frac{e}{r}$

$$\ddot{x_r} + \omega_x^2(x_r + e_r\theta) = 0 \tag{A2c}$$

Equation of rotational equilibrium (taking moment about CM)

$$J\ddot{\theta} + K_x(x + e\theta)e + K_t\theta = 0 \tag{A3a}$$

$$Mr^2\ddot{\theta} + K_x\left[(x + e\theta)e + \frac{K_t}{K_x}\theta\right] = 0 \tag{A3b}$$

Divide both sides of equation by M and r^2 and given that $\omega_x^2 = \frac{K_x}{M}$

$$\ddot{\theta} + \omega_x^2\left[\left(\frac{x}{r} + \frac{e}{r}\theta\right)\frac{e}{r} + \frac{b^2}{r^2}\theta\right] = 0 \tag{A3c}$$

Given that $b_r = \frac{b}{r}$

$$\ddot{\theta} + \omega_x^2[(x_r + e_r\theta)e_r + b_r^2\theta] = 0 \tag{A3d}$$

$$\ddot{\theta} + \omega_x^2[(e_r)x_r + (b_r^2 + e_r^2)\theta] = 0 \tag{A3e}$$

Recall the reduced equations of dynamic equilibrium

$$\begin{bmatrix}1 & 0\\ 0 & 1\end{bmatrix}\begin{Bmatrix}\ddot{x_r}\\ \ddot{\theta}\end{Bmatrix} + \omega_x^2\begin{bmatrix}1 & e_r\\ e_r & b_r^2 + e_r^2\end{bmatrix}\begin{Bmatrix}x_r\\ \theta\end{Bmatrix} = \begin{Bmatrix}0\\ 0\end{Bmatrix} \tag{A4a}$$

$$\omega_x^2\begin{bmatrix}1 & e_r\\ e_r & b_r^2 + e_r^2\end{bmatrix}\begin{Bmatrix}x_r\\ \theta\end{Bmatrix} - \Omega_j^2\begin{bmatrix}1 & 0\\ 0 & 1\end{bmatrix}\begin{Bmatrix}x_r\\ \theta\end{Bmatrix} = \begin{Bmatrix}0\\ 0\end{Bmatrix} \tag{A4b}$$

Where $\Omega_{j=1,2}$ are the natural angular velocities of the coupled modes of vibration (i.e., the *eigenvalues*)

Let $\lambda_j^2 = \frac{\Omega_j^2}{\omega_j^2} \Rightarrow Det\begin{vmatrix} 1-\lambda_j^2 & e_r \\ e_r & (b_r^2+e_r^2)-\lambda_j^2 \end{vmatrix} = 0 \Rightarrow$

$$\left(1-\lambda_j^2\right)\left[(b_r^2+e_r^2)-\lambda_j^2\right]-e_r^2 = 0 \tag{A4c}$$

Solution for values of λ_j^2 can be obtained by solving the roots of a quadratic equation.

It can be shown using the elementary expression: $\frac{-b\pm\sqrt{b^2-4ac}}{2a}$ that

$$\lambda_j^2 = \frac{1+(b_r^2+e_r^2)}{2} \pm \sqrt{\left[\frac{1-(b_r^2+e_r^2)}{2}\right]^2 + e_r^2} \tag{A4d}$$

Solution for the eigenvector is accordingly obtained as follows

$$\begin{bmatrix} 1-\lambda_j^2 & e_r \\ e_r & (b_r^2+e_r^2)-\lambda_j^2 \end{bmatrix}\begin{Bmatrix} x_r = 1 \\ \theta_j \end{Bmatrix} = \begin{Bmatrix} 0 \\ 0 \end{Bmatrix} \Rightarrow \tag{A5a}$$

$$\left(1-\lambda_j^2\right) + e_r\,\theta_j = 0 \;\Rightarrow\; \theta_j = \frac{\lambda_j^2-1}{e_r} \quad \text{or } \theta_j = \frac{\lambda_j^2-1}{\frac{e}{r}} \tag{A5b}$$

Appendix B

Calculation of effective displacement, mass, stiffness and natural period of the TB model

$F_b = S_d(T_1)\lambda m$

Mass, $m = 5{,}816$ tonnes

$F_b = 0.23\text{g}(0.85)5816 = 11153$ kN

λ is taken as 0.85

Distribution of base shear

$F_i = F_b \frac{z_i m_i}{\sum_i z_i m_i}$

$\delta_{eff} = \left(\frac{\sum m_i\delta_i^2}{\sum m_i\delta_i}\right) = \frac{4191047785}{1.33\text{E+}08} \approx 31$ mm

$m_{eff} = \left(\frac{(\sum m_i\delta_i)^2}{\sum m_i\delta_i^2}\right) = 4244$ tonnes

$k_{eff} = \left(\frac{F_b}{\delta_{eff}}\right) = \frac{11153}{31} = 354924$ kN/m $\qquad T_{eff} = 2\pi\sqrt{\left(\frac{m_{eff}}{k_{eff}}\right)} = 0.7$ s

Level	m_i (kg)	z_i (m)	$m_i z_i$	F_i (kN)	δ_i	$m_i \delta_i^2$	$m_i \delta_i$
8	675359	26.2	17694406	2293.627	45	1367601975	30391155
7	719185.4	23	16541264	2144.151	39	1093880993	28048231
6	719185.4	19.8	14239871	1845.835	32.7	769017756.4	23517363
5	719185.4	16.6	11938478	1547.518	26.1	489916286.3	18770739
4	751277.5	13.4	10067119	1304.944	19.6	288610764.4	14725039
3	737925	10.2	7526835	975.6614	13.3	130531553.3	9814403
2	737925	7	5165475	669.5715	7.7	43751573.25	5682023
1	755555	3.8	2871109	372.1658	3.2	7736883.2	2417776
sum	5815598		86044556	11153.47		4191047785	1.33E+08

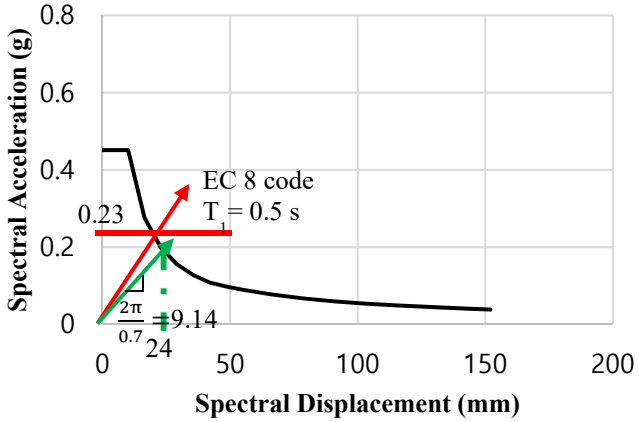

Level	δ_i (mm) by Code lateral force method	δ_i (mm) by Generalised Force method (=24/32×d_i)
8	45	34
7	39	29
6	32.7	24
5	26.1	20
4	19.6	15
3	13.3	10
2	7.7	6
1	3.2	2

Appendix C

Determination of eccentricity, torsional stiffness and edge displacement ratio of the TU model

Step 1: Finding the location of the CR of torsionally unbalanced building

Apply lateral load at the location of centre of mass of the building.
Find values of δ and ϕ based on results of static analysis by the computer model of the building

X_{CM}=31.04 m

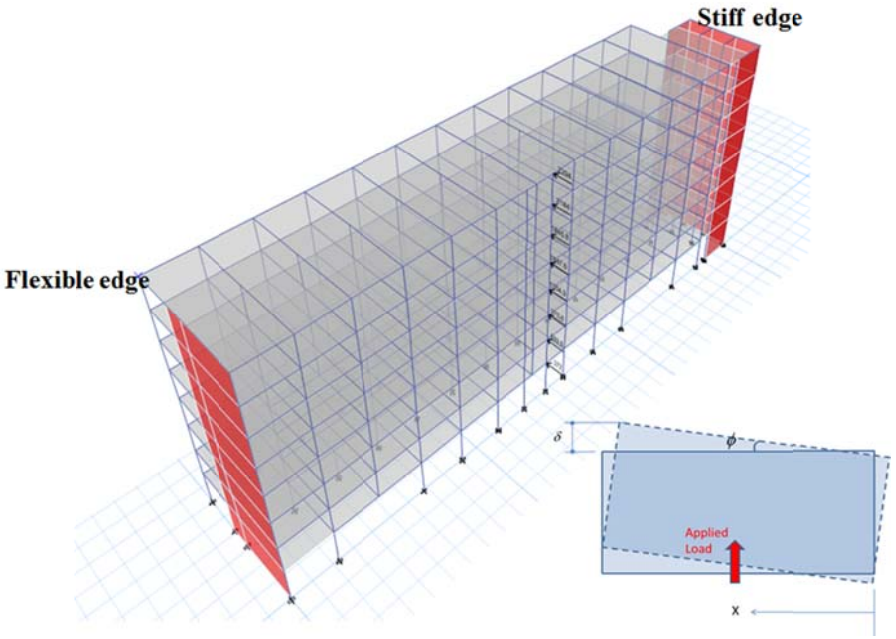

						Flexible edge			Stiff edge	
Level	m_i (kg)	z_i (m)	$m_i z_i$	F_i (kN)	δ_i(mm)	$m_i \delta_i^2$	$m_i \delta_i$	δ_i(mm)	$m_i \delta_i^2$	$m_i \delta_i$
8	684387	26.2	17930951	2320	76	3932243793	51876567	33	727339585	22311030
7	728214	23	16748923	2166	65	3067244903	47261092	29	591491870	20754101
6	719185	19.8	14239871	1842	54	2066190887	38548337	24	417710072	17332368
5	719185	16.6	11938478	1544	42	1280754128	30349624	20	273470248	14024115
4	751278	13.4	10067119	1302	31	726643111	23364730	15	164559824	11118907
3	737925	10.2	7526835	974	21	313145853	15201255	10	78286463	7600628
2	737925	7	5165475	668	12	97590581	8486138	6	27458189	4501343
1	755555	3.8	2871109	371	4	14627545	3324442	3	5107552	1964443
sum	5833655		8688760			11498440801	218412186		2285423804	99606934

Flexible edge

$$\delta_{eff} = \left(\frac{\Sigma m_i \delta_i^2}{\Sigma m_i \delta_i}\right) = \frac{11498440801}{218412186} \approx 52.6 \text{ mm}$$

Stiff edge

$$\delta_{eff} = \left(\frac{\Sigma m_i \delta_i^2}{\Sigma m_i \delta_i}\right) = \frac{2285423804}{99606934} \approx 22.9 \text{ mm}$$

$$\phi = \left(\frac{\Sigma m_i \delta_i^2}{\Sigma m_i \delta_i}\right) = \frac{(52.6 - 22.9)}{(60.44 \times 1000)} \approx 0.00049$$

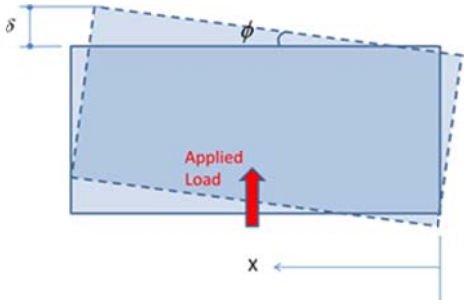

Step 1: Finding the location of the CR of torsionally unbalanced building continued

Apply a second lateral load at an arbitrary location which is further away from the centre of mass of the building (here the load is applied 0.05L from the CM).

Find values of δ_2 and ϕ_2 based on results of static analysis by the computer model of the building

$$X_{CM} + 0.05L = 34.04 \text{ m}$$

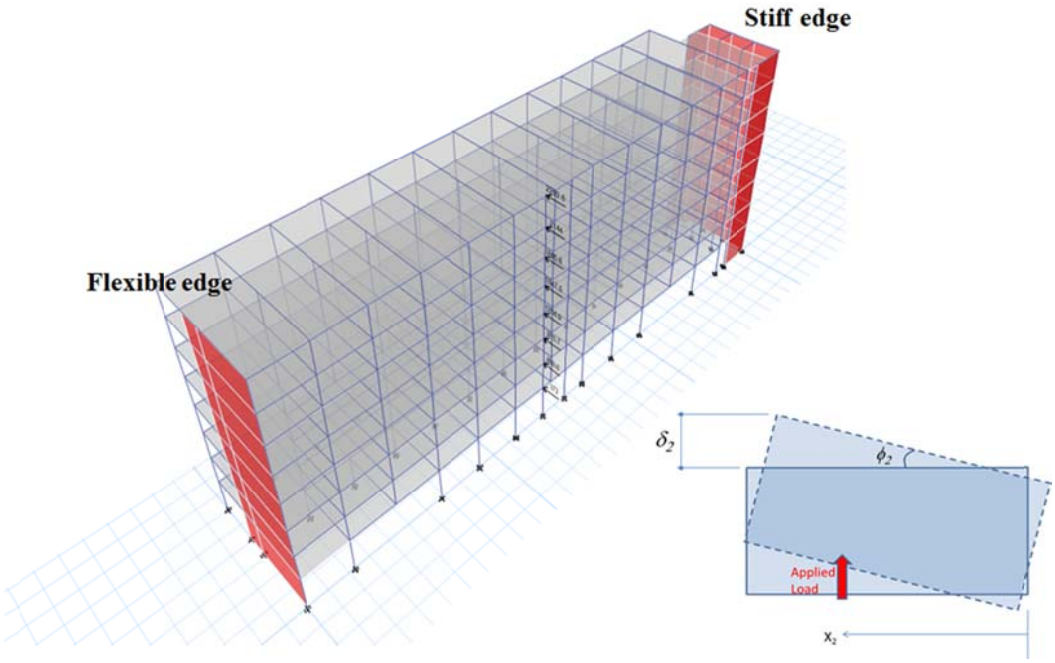

						Flexible edge		Stiff edge		
Level	m_i (kg)	z_i (m)	$m_i z_i$	F_i (kN)	δ_i (mm)	$m_i \delta_i^2$	$m_i \delta_i$	δ_i (mm)	$m_i \delta_i^2$	$m_i \delta_i$
8	684387	26.2	17930951	2320	83	4737494043	56941034	29	583536098	19984113
7	728214	23	16748923	2166	71	3702014535	51921662	26	477242366	18642280
6	719185	19.8	14239871	1842	58	2495005182	42360020	22	335543140	15534405
5	719185	16.6	11938478	1544	46	1541710550	33298284	17	217740572	12513826
4	751278	13.4	10067119	1302	34	873592990	25618563	13	132893477	9991991
3	737925	10.2	7526835	974	22	376902573	16677105	9.2	62457972	6788910
2	737925	7	5165475	668	12	117152973	9297855	5.5	22322231	4058588
1	755555	3.8	2871109	371	4	17407987	3626664	2.4	4351997	1813332
sum	5833655		8688760		0	13861280833	239741188		1836087854	89327444

Flexible edge

$$\delta_{eff} = \left(\frac{\Sigma m_i \delta_i^2}{\Sigma m_i \delta_i}\right) = \frac{13861280833}{239741188} \approx 57.8 \text{ mm}$$

Stiff edge

$$\delta_{eff} = \left(\frac{\Sigma m_i \delta_i^2}{\Sigma m_i \delta_i}\right) = \frac{1836087854}{89327444} \approx 20.6 \text{ mm}$$

$$\phi = \left(\frac{\Sigma m_i \delta_i^2}{\Sigma m_i \delta_i}\right) = \frac{(57.8 - 20.6)}{(60.44 \times 1000)} \approx 0.00062$$

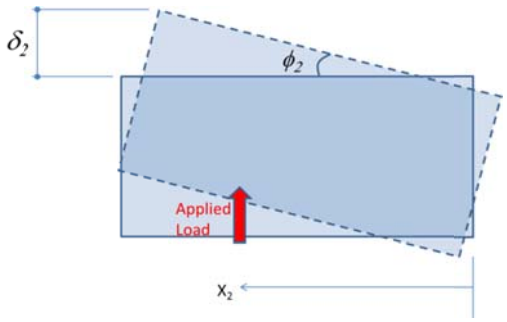

Step 2: Finding eccentricity (e_r) and torsional stiffness (b_r)

Given the value of ϕ and ϕ_2 the value of eccentricity e can be found by extrapolation

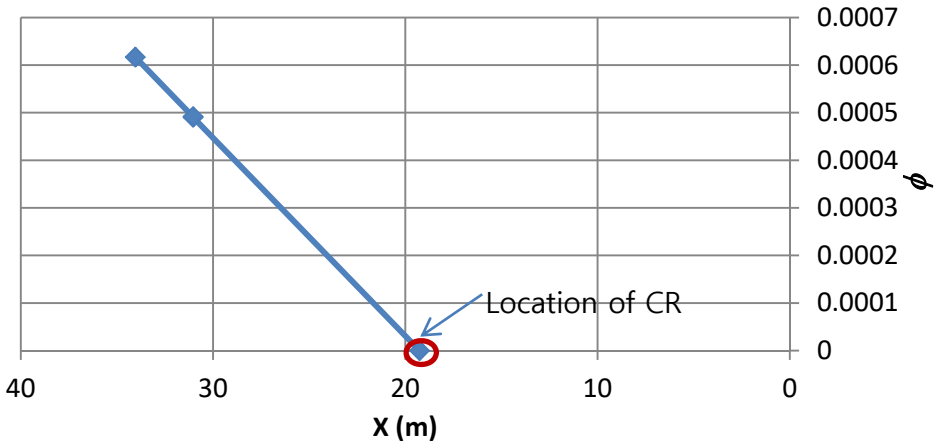

$$e = 34.04 - 19.3$$
$$= 11.8 \text{ m}$$
$$r = \sqrt{\frac{60.44^2 + 12.2^2}{12}} = 17.8 \text{ m}$$
$$e_r = 0.65$$

Given the value of δ, δ_2 and e find the value of Δ_o which corresponds to the displacement demand when the lateral load is applied at the centre of stiffness of the building.

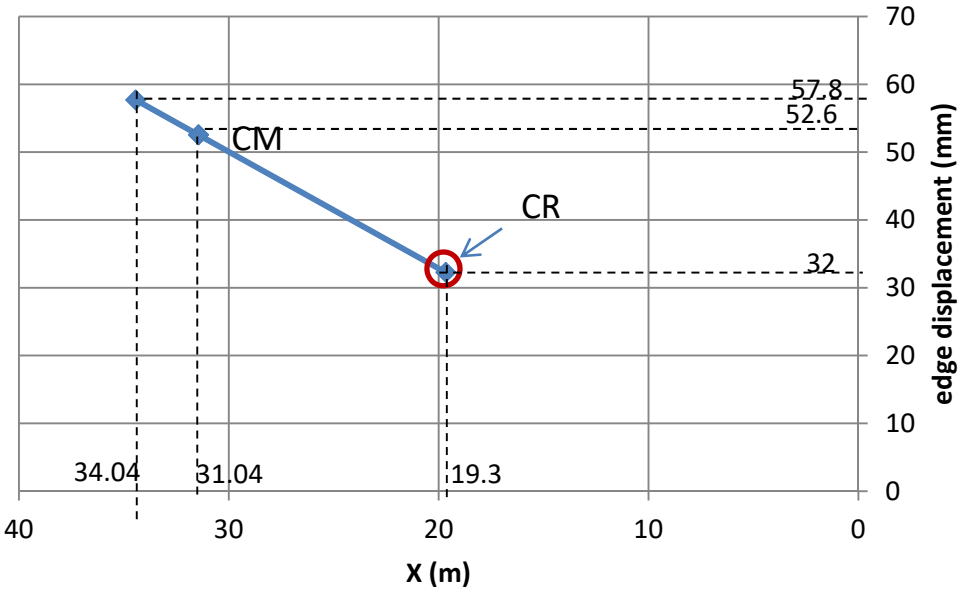

$\Delta = 52.5$ mm, $\Delta_o = 32$ mm

$\frac{\Delta}{\Delta_o} = 1.6$

Step 2: Finding eccentricity (e_r) and torsional stiffness (b_r) continued

Take Δ=δ when the load is positioned at e/r(e_r)=0.65
Result is Δ/Δ_o=1.6, B_r(=B/r)=1.68
Find value of b_r (= b/r) using Eq. (9)

$$\frac{\Delta}{\Delta_o} = 1 + \frac{e_r}{b_r^2} B_r$$

$$b_r = \sqrt{\frac{e_r B_r}{\left(\frac{\Delta}{\Delta_o} - 1\right)}} = 1.35$$

Result is b/r = 1.35
Find λ_j using Eq. (4b)

$$\lambda_j^2 = \frac{1 + (b_r^2 + e_r^2)}{2} \pm \sqrt{\left[\frac{1 - (b_r^2 + e_r^2)}{2}\right]^2 + e_r^2}$$

$$\lambda_1 = 0.85, \quad \lambda_2 = 1.59$$

Find θ_j using Eq. (8d)

$$\theta_j = \frac{\lambda_j^2 - 1}{e_r} .$$

$$\theta_1 = -0.43, \quad \theta_2 = 2.34$$

Find the displacement ratio using Eq. 13(c)

$$\frac{\Delta}{\Delta_0} = \frac{x_{\pm B}(\max)}{RSD(T, \xi)} = \sqrt{\sum_{j=1}^{2} \left[\frac{1 + \theta_j(\pm B_r)}{1 + \theta_j^2} \times \frac{1}{\lambda_j}\right]^2}$$

For the flexible edge $\frac{\Delta}{\Delta_0}$ = 1.73, for the stiff edge $\frac{\Delta}{\Delta_0}$ = 0.55